Documentation of weather regime ensemble forecasts

for operational ECMWF IFS medium-range (0-15 days) and extended-range (0-45 days)

by Helmholtz Young Investigator group "Sub-seasonal Atmospheric Predictability: Understanding the role of Diabatic Outflow" (SPREADOUT).

Author: Christian M. Grams, Institute for Meteorology and Climate Research (IMK-TRO), Karlsruhe Institute of Technology (KIT), Postbox 3640, 76021 Karlsruhe, Germany, grams@kit.edu, +49 721 608 26544.

Date: 30 January 2019

Contents

Summary 1
1. Background on the seven Atlantic-European weather regimes 2
2. Ensemble forecast products 5
Medium-range ensemble (0-15days) 5
Extended-range (0-45days) ensemble 9
3. Technical Implementation 11
Weather regime definition 11
NAO index 12
Attribution of ensemble forecast members to weather regimes 11
Appendix 1: Modulation of surface weather 12
Winter anomalies 13
Spring anomalies 18
Summer anomalies 23
Autumn anomalies 28
Appendix 2: Modulation of surface weather in the Alpine Region 32
References 41

Summary

Weather regimes are quasi-stationary, recurrent, and persistent states of the large-scale extratropical circulation that describe most of the multi-day variability in the Atlantic-European region.
Based on the operational ECMWF IFS medium-range (0-15 days, 2x per day) and extended-range (0-45 days, 2x per week) ensemble, forecast products for European weather regime are produced by the Helmholtz YIG SPREADOUT at KIT and hosted at ETH Zurich by the Atmospheric Dynamics group. The forecast products employ an extended year-round definition of 7 weather regimes, that proved to be useful for applications in e.g. the energy sector (Grams et al. 2017). From a forecasting perspective the modulation of surface weather for multi-day periods by weather regimes is of interest. This modulation has been documented for 100m wind (Grams et al. 2017), moisture transport and heavy precipitation (Pasquier et al. 2019), heat waves (Schaller et al. 2018), and marine cold air outbreaks (Papritz and Grams 2018).
This documentation gives background on the 7 weather regimes, their mean flow characteristics, and their modulation of surface weather for different seasons. Available forecast products are explained before giving the essential background on the technical implementation. Parts of this documentation are taken from the Supplemental Materials of Grams et al. (2017).

1. Background on the seven Atlantic-European weather regimes

Here a meteorological perspective on the seven weather regimes is given based on 500 hPa geopotential height (*Z500*, **Figure 1**) and monthly weather regime frequencies (**Figure 2**). For comparison with other classifications (Michel and Rivière 2011; Ferranti et al. 2015) absolute values of year-round *Z500* are shown without normalisation. Although the flow patterns are comparable in all seasons, season-specific *Z500* are shown in the **Appendix 1: Modulation of surface weather** along with seasonal surface weather anomalies.
The "no regime" conditions are representative of the climatological mean (not shown) and exhibit no distinct anomalies in *Z500* (*Z500'*, shading in **Figure 1h**). The absolute *Z500* field (contours in **Figure 1h**) is characterised by a climatological trough over North America, and weak ridging over the eastern North Atlantic and western Europe. Strong westerly upper-level flow, parallel to the isohypses of geopotential height (contours in **Figure 1h**), prevails in the eastern and central North Atlantic, and reaches into Europe.

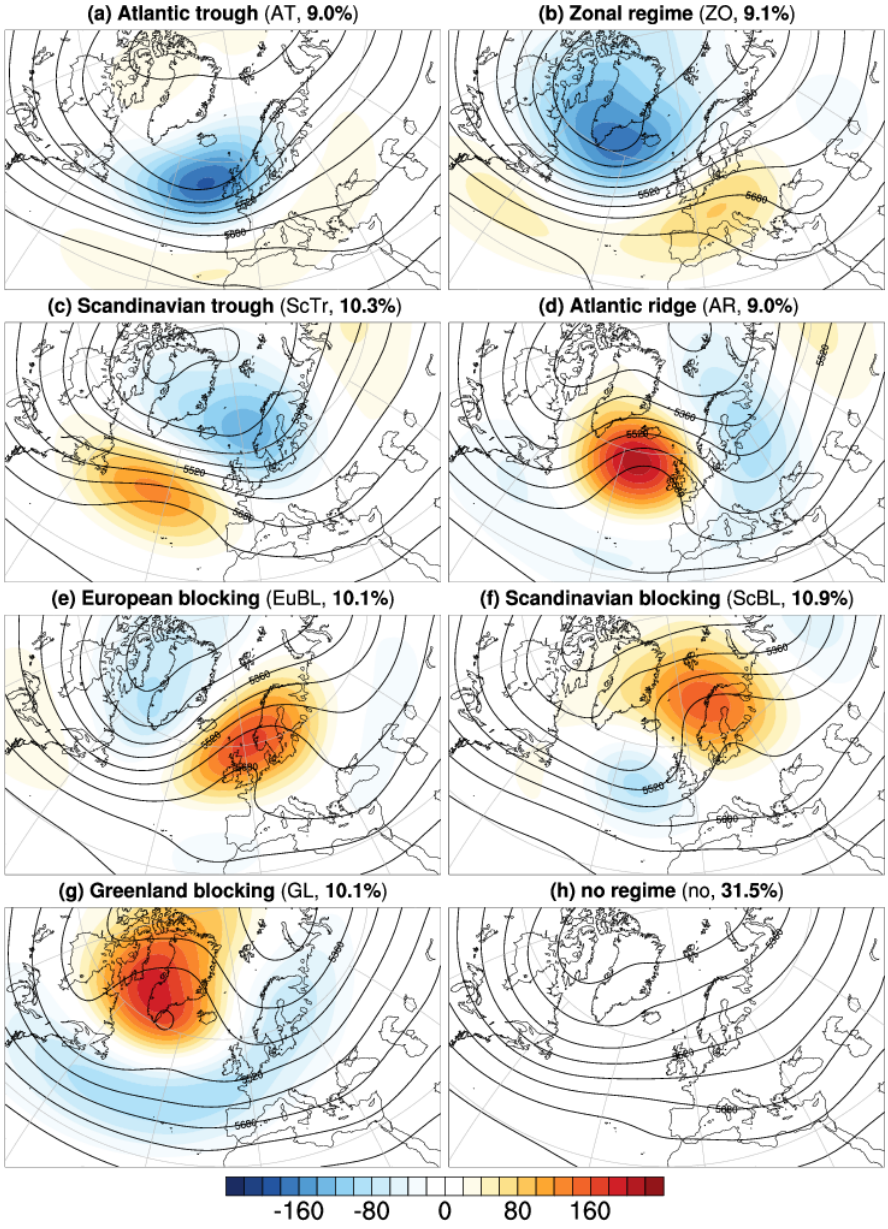

Figure 1: Atlantic European weather regimes. Mean low-pass filtered (10 days) 500 hPa geopotential height anomaly (*Z500'*, shading, every 20 geopotential meters), and mean absolute 500 hPa geopotential height (*Z500*, black contours, every 40 geopotential meters) for all days in ERA-Interim (1979-2015) attributed to one of the 7 weather regimes (a-g) and to no regime (h). Although the regime definition is based on normalised data, here non-normalised data are shown. Regime name, abbreviation, and relative frequency (all year in percent) indicated in the sub-figure caption.

The seven weather regimes are deviations from these climatological mean conditions. We consider three of the seven weather regimes as cyclonic (AT, ZO, ScTr, **Figure 1a-c**) since the predominant signature is a negative *Z500* anomaly. The regimes ZO and ScTr are flanked by moderate positive *Z500* anomalies over Europe and the North Atlantic, respectively (**Figure 1b-c**). Four regimes are considered as blocked (AR, EuBL, ScBL, GL, **Figure 1d-g**) since their dominant feature is a strong positive *Z500* anomaly flanked by weaker negative anomalies.

Table 1: Mean NAO index during the seven weather regimes and seasonal frequencies. Top: Mean NAO index during the seven weather regimes in different seasons. See Methods for details of computation. Bottom: Seasonal frequencies in percent.

season	**AT**	**ZO**	**ScTr**	**AR**	**EuBL**	**ScBL**	**GL**	**no**
DJF	+0.40	+0.99	+0.88	-0.22	+0.26	-0.18	-0.84	+0.23
MAM	-0.04	+1.02	+0.60	-0.20	+0.65	0.01	-0.93	+0.13
JJA	-0.51	+0.83	+0.43	-0.19	+0.70	-0.36	-1.31	+0.00
SON	-0.35	+0.88	+0.19	-0.36	+0.66	-0.33	-1.52	-0.03
DJF	13.1%	13.8%	11.3%	9.75	10.9%	6.5%	11.7%	23.0%
MAM	7.5%	10.8%	11.0%	7.55	8.7%	9.1%	13.1%	32.3%
JJA	7.5%	3.5%	5.8%	6.6%	12.2%	16.0%	9.1%	39.3%
SON	8.0%	8.3%	13.3%	12.1%	8.7%	11.9%	6.3%	31.3%

The **Atlantic trough** regime (AT) features a single dominant negative *Z500* anomaly east of Ireland (**Figure 1a**). The upper-level flow is straight westerly between 40-50°N across the entire North Atlantic and into Europe (contours in **Figure 1a**). Due to the negative *Z500* anomaly located between Iceland and the Azores, the NAO index is positive in winter (+0.40) during AT but not in other seasons (**Table 1**).

The **Zonal regime** (ZO) is dominated by a negative *Z500* anomaly around Iceland and southern Greenland, and by weakly blocked conditions over western continental Europe due to an enhanced ridge (**Figure 1b**). It constitutes the actual positive phase of the NAO (NAO index strongly positive during ZO in all seasons, **Table 1**). Compared to AT the negative anomaly is shifted poleward. Westerly upper-level flow prevails in the eastern North Atlantic and turns into southwesterly flow over the North Sea region and into Scandinavia (contours in **Figure 1b**).

During the **Scandinavian trough** regime (ScTr), the negative *Z500* anomaly is shifted eastward compared to ZO and a broad trough extends into northern and eastern Europe (**Figure 1c**). At the same time a positive *Z500* anomaly reflects weak ridging over the North Atlantic between 40-50°N. The prevailing upper-level westerly flow is shifted northward compared to AT (contours in **Figure 1c**). ScTr is NAO positive in all seasons (**Table 1**).

A strong positive *Z500* anomaly resides south of Iceland during the **Atlantic ridge** regime (AR) accompanied by a blocking ridge west of Ireland and a trough affecting wide parts of Europe (**Figure 1d**). The usually prevailing westerly flow is blocked and deflected around the ridge turning into northwesterlies over Northern and Western Europe (contours in **Figure 1d**). The NAO is weakly negative in all seasons (**Table 1**).

During the **European blocking** regime (EuBL) a positive *Z500* anomaly is centred over the North Sea region and a blocking ridge expands over Western and Central Europe (**Figure 1e**). At the same time an upstream trough extends over the Labrador Sea and a downstream trough over Southeastern Europe (contours in **Figure 1e**). The upper-level flow is strongly deflected into southwesterlies from Newfoundland over Iceland to northern Scandinavia. This flow configuration projects to the positive (!) phase of the NAO in all seasons (**Table 1**).

During **Scandinavian blocking** (ScBL) the positive *Z500* anomaly is shifted into northern Scandinavia accompanied by a weaker negative anomaly in the eastern North Atlantic and

Western Europe (**Figure 1f**). The upper-level flow is split with a branch deflected poleward around the blocking anticyclone and westerly flow over Iberia and the Mediterranean (contours in **Figure 1f**). The NAO index is weakly negative in all seasons but spring (**Table 1**).

Greenland blocking (GL) constitutes the negative phase of the NAO (strongly negative NAO index in all seasons **Table 1**). It features a strong positive *Z500* anomaly over Greenland and a zonally aligned negative anomaly stretching from the eastern North Atlantic into Northern Europe (**Figure 1g**). The prevailing westerly flow is deflected southward, centred around 40°N, and extends into the Mediterranean. Northern Europe is affected by northerly upper-level flow (contours in **Figure 1g**).

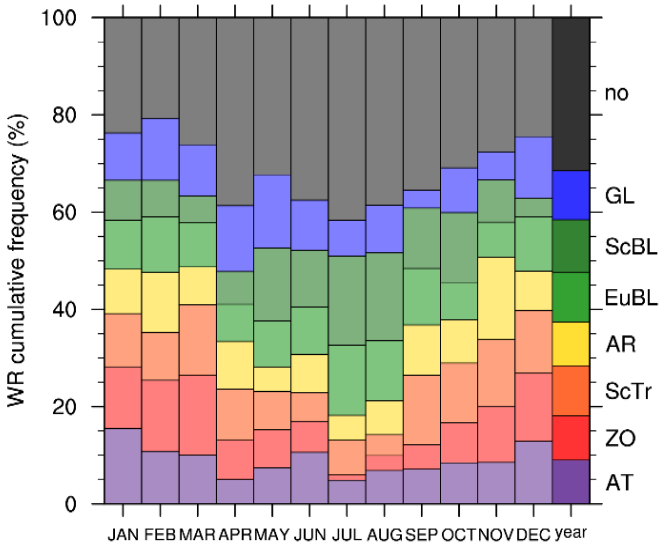

Figure 2: Relative frequencies of the 7 weather regimes. Cumulative relative frequency (in percent) of days classified into one of the seven regimes or no regime for each month during 1979-2015 (light colours) and the entire year (dark colours, last column). Regime abbreviations on the right.

The mean NAO indices for the seven regimes show some seasonal variability (**Table 1**). This is also due to the fact that the NAO index used here is based on the monthly varying leading EOF pattern; whereas our weather regime definition is based on year-round constant EOF patterns (see **Technical Implementation in Section 3**). Still it is striking that zonal regimes do not simply project into positive NAO neither do blocked regime only project into NAO negative.

From this overview of the seven weather regimes in winter and their mean NAO indices we conclude that the NAO alone does not account for the full range of large-scale flow variability in the Atlantic-European region and a mere interpretation of surface weather based on the NAO index would be misleading (Jerez and Trigo 2013; Santos et al. 2016; Zubiate et al. 2017). In contrast, our seven weather regimes reflect the seasonal variability of the preferred states of the large-scale midlatitude circulation in the Atlantic European region (**Figure 2**). All seven regimes share an equal annual frequency of 9 to 11% (right bar in **Figure 2**); while 31.5% of all days are attributed to no regime (grey in **Figure 2**, ranging from 20.7% in December to 41.7% in July).

In general, cyclonic regimes (AT, ZO, ScTr) are more frequent in winter months (November to March, **Figure 2**), in particular ZO. Summer months (May to September) are more frequently associated with blocked regimes (AR, EuBL, ScBL, GL, **Figure 2**), with a dominance of ScBL. Of the cyclonic regimes, AT occurs year-round, and is the preferred cyclonic regime in summer. In contrast, ZO and ScTr are more frequent in winter and in the transition seasons and almost absent in summer. Of the blocked regimes, GL occurs year-round. The two blocked regimes over Europe (EuBL and ScBL), albeit generally more frequent in summer, show opposite

behaviour in relative seasonal preference. Whereas EuBL is the preferred blocking in Europe in core winter (EuBL 10.9% vs. ScBL 6.5%; **Figure 2**), ScBL occurs more frequently than EuBL in core summer (EuBL 12.2% vs. ScBL 16.0%, **Figure 2**). Finally, AR occurs more frequently in winter (9.7%) than summer (6.6%, **Figure 2**).

2. Ensemble forecast products

Medium-range ensemble (0-15 days)

A compact overview of weather regime activity according to the ensemble forecast is given by the plot "**Weather regimes**" (**Figure 3**). Stacked bars show the relative number of ensemble members (including CF) attributed to a specific regime at each forecast step based on the maximum projection in one of the 7 regimes. This maximum projection must occur in a period during which the projection is above a specified threshold (persistence criterion; see **Section 3 Technical Implementation**). Days with a weak maximum projection are attributed to no regime (grey). Below the bar plots three rows show the attribution of the ensemble mean, control, and high resolution (up to 240h) forecasts. The plot variant "**WR SimpleLC**" does not apply a persistence criterion (instantaneous attribution) but requires the maximum projection to be above the specified threshold. The plot variant "**WR maxIWR**" attributes each member according to the maximum projection in a regime, without filtering out weak projections (no "no regime"; not shown). For the example forecast of 00 UTC 28 January 2019 (**Figure 3**), the forecast starts during an active Scandinavian Trough regime. After a period of rather no regime, it is very likely that a Scandinavian Blocking emerges around 3 February 2019.

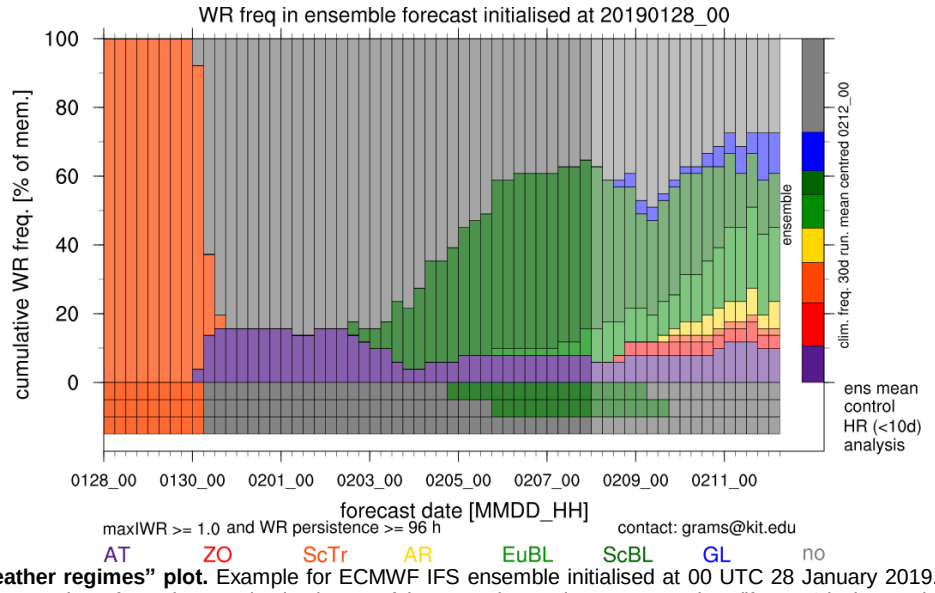

Figure 3: "Weather regimes" plot. Example for ECMWF IFS ensemble initialised at 00 UTC 28 January 2019. Stacked bars show the relative number of members projecting in one of the 7 weather regimes or no regime (if I_{wr}<1.0 is the maximum projection and within a 96h period of I_{wr}<1.0). The 3 bottom rows show the attribution of the ensemble mean, control, and high resolution (up to 240h) forecasts, respectively. The last 96h are shown in pale colours as the persistence criterion is less strict (see Section 3).

The plot **"WR Members"** shows the actual sequence of weather regimes for the individual members, which is hidden in the compact overview of the "Weather Regimes" plot (**Figure 4**). It reveals that indeed some members transition from Scandinavian Trough into an Atlantic Trough regime, but for most members a Scandinavian Blocking emerges after a period of no regime. These plots are complemented by the plot **"WR Index"** showing the distribution of the normalised projection (weather regime index Iwr) of the ensemble forecast in each of the seven regimes and at each forecast time step (**Figure 5**). It helps interpreting the overview given by

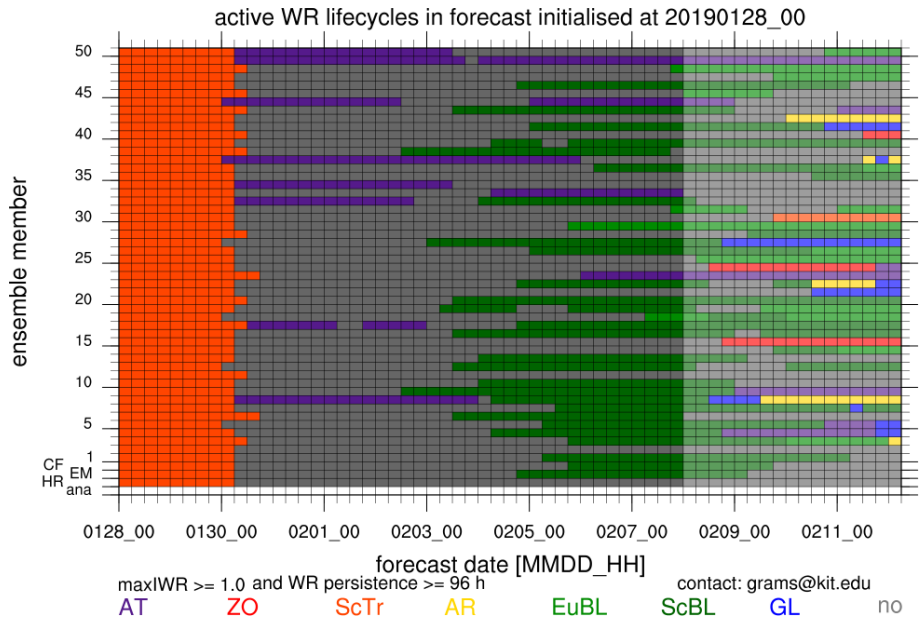

Figure 4: "WR Members" plot. The currently active weather regime in each member is shown (maximum projection I_{wr} > 1.0 and embedded in an at least 96h period of I_{wr} > 1.0) at each forecast step. The last 96h are shown in pale colors as the persistence criterion becomes less strict (see Section 3).

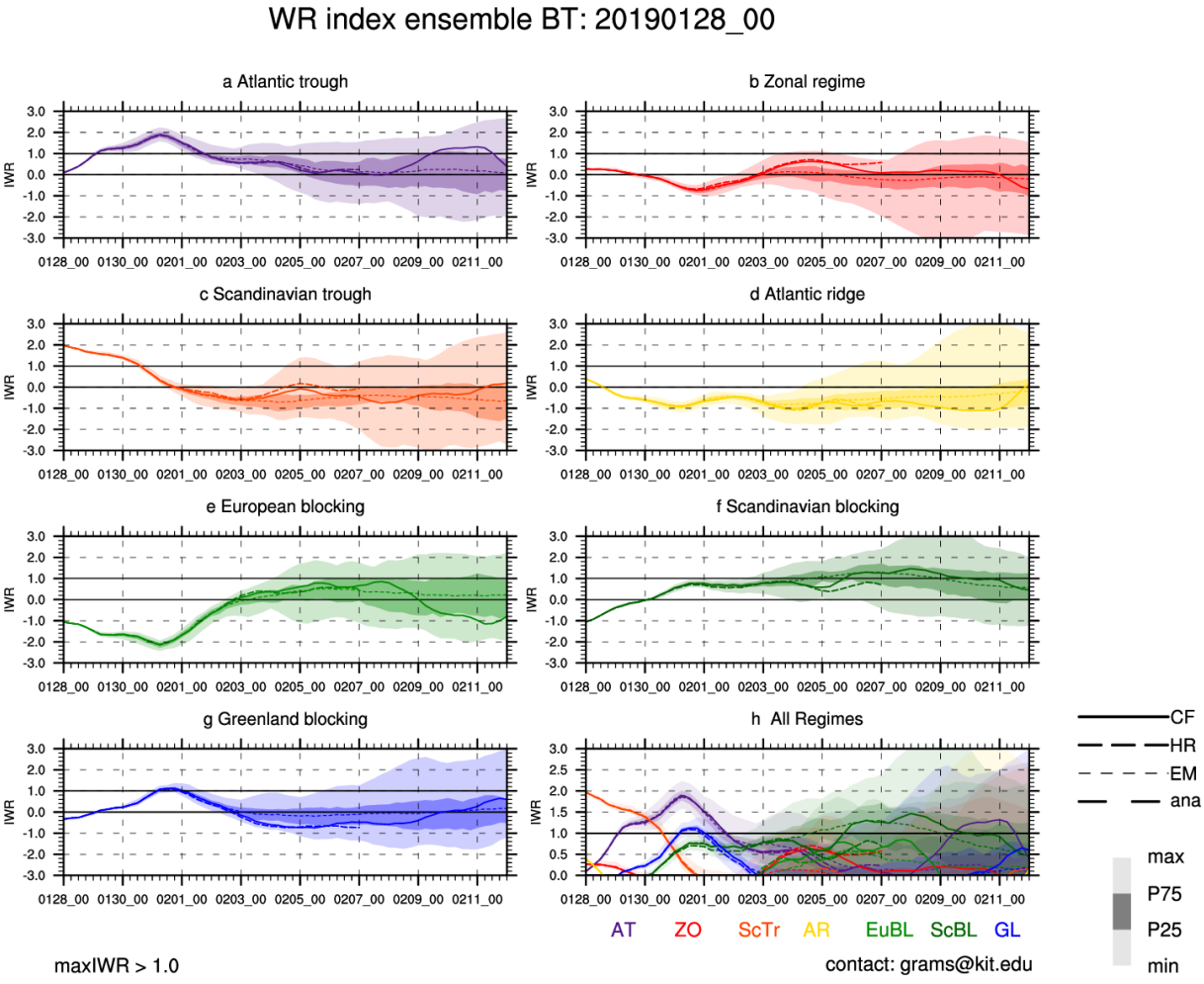

Figure 5: "WR index" plot. Panels a-g show the distribution of the respective weather regime index I_{wr} at each forecast step. Light shades show the bounds given by the members with the maximum and minimum projection, dark shades show the 75th and 25th percentile. Lines show the projection of the control forecast (bold solid), high resolution forecast (bold dashed, only up to 240h), and ensemble mean (thin dashed). The last panel h compares all projections by zooming only on positive values.

the plot "Weather regimes" by allowing to assess the strength of the projection. For the example forecast, we see that the strong projection into Scandinavian Trough decays until 3 February. Scandinavian Blocking will most likely establish after 3 February. During the transition phase (30 January - 2 February) Atlantic Trough shows a strong projection, but only in few members it remains persistent for at least 96h and thus fulfils the criteria to be marked as an active regime in "Weather Regimes" and "WR Members".
The combination of the plots, **"Weather regimes", "WR index"**, **and "WR Members"**, give a handy tool for a very quick overview of the weather regime activity in the ensemble forecast and of the intensity of the projection into the regimes.

Some additional plots help exploring in more detail the current characteristics of the regimes in the ensemble.
The plot **"Z500 clim"** shows the climatological mean 500hPa Geopotential height based on ERA-Interim. It is helpful to compare this to the current configuration of 500 hPa Geopotential height shown in the plot "**Z500 mean**" (example **Figure 6**). The latter shows the mean *Z500* of all ensemble members attributed to the respective regime (attribution including persistence as shown in "Weather Regimes" and "WR Members") and also lists (as text) all members attributed to each regime. In addition, the plot "**Z500 std**" shows the standard deviation amongst the members attributed to the respective regime (not shown). The mean or standard deviation are only computed if at least 4 members are attributed to the respective regime. For the example forecast initialised at 00 UTC 28 January 2019 we briefly discuss the valid time 00 UTC 11 February 2019 (**Figure 6**). 11 ensemble members each project into EuBL or ScBL (**Figure 6e,f**). However, the ridge for EuBL extends farther into Scandinavia compared to the

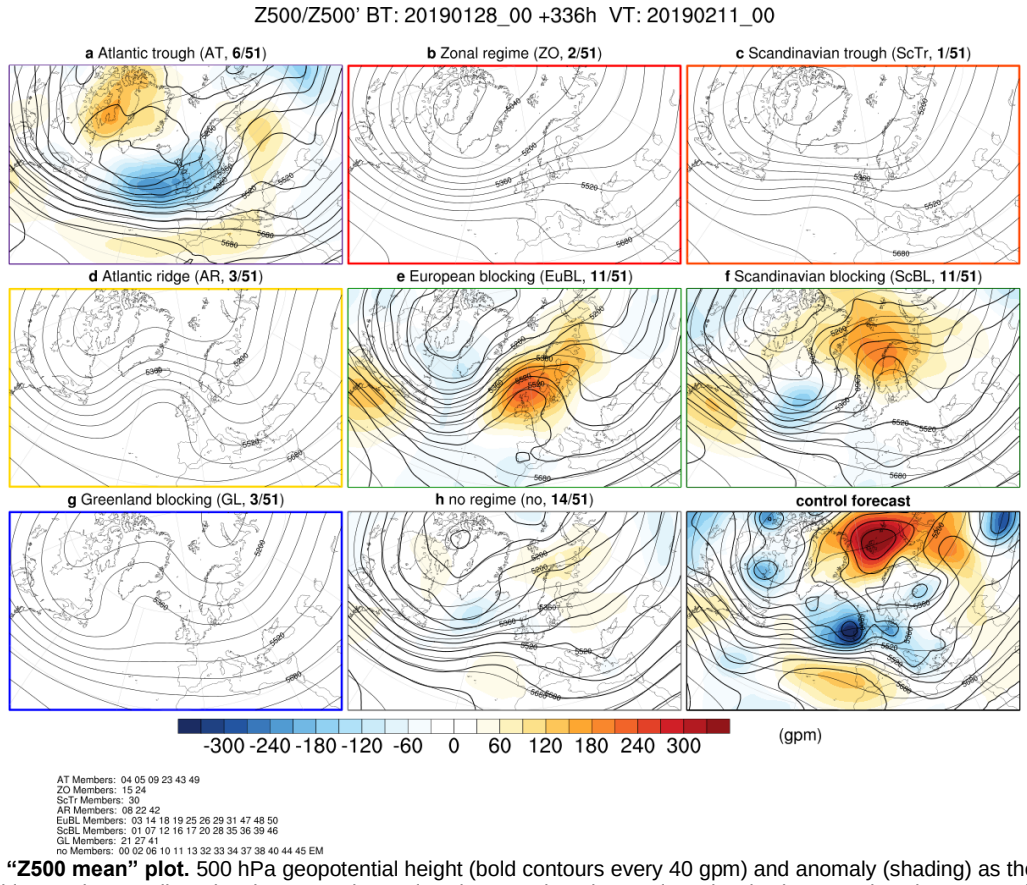

Figure 6: "Z500 mean" plot. 500 hPa geopotential height (bold contours every 40 gpm) and anomaly (shading) as the mean of all ensemble members attributed to the respective regime (see numbers in panel captions). The mean is only computed if at least 4 members are attributed. Thin contours show the climatological mean geopotential height (every 40 gpm) in the respective regime based on ERA-Interim (1979-2015) data. The text below the plot lists the members attributed to each regime; EM for ensemble forecast, 00 for control forecast, HR for high resolution forecast.

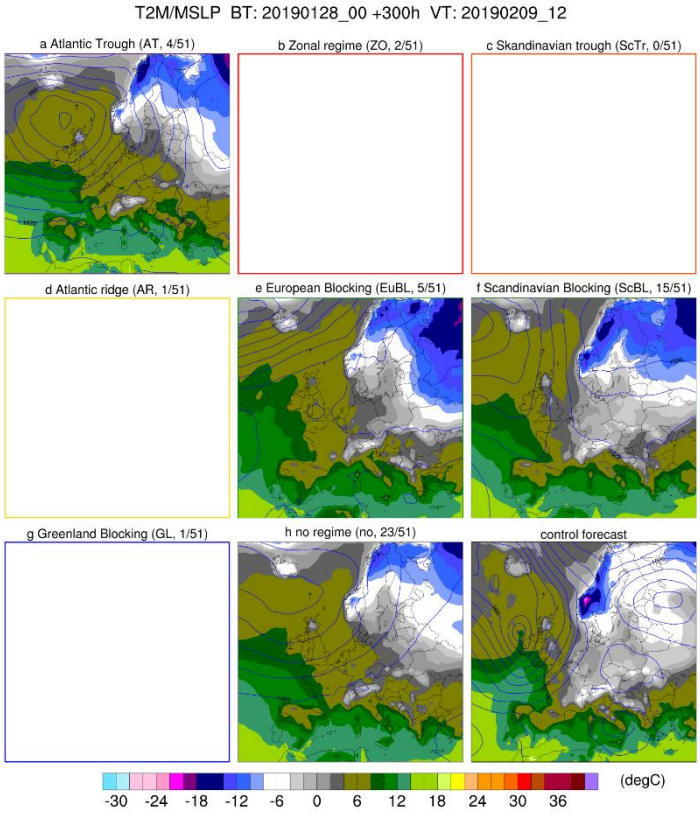

Figure 7: "T2m" plot. 2m temperature (shading every 2°C) and mean sea level pressure (contours every 5hPa) as the mean of all ensemble members attributed to the respective regime (see numbers in panel captions). The mean is only computed if at least 4 members are attributed.

climatological mean configuration of EuBL (cf. thin and thick contours in **Figure 6f**). Other members project into the AT regime but still exhibit a ridge over Russia and Greenland. Thus, the plot "Z500 mean" helps to understand the current configuration of the regimes and into which scenarios the large-scale flow might evolve.

Similar to "Z500 mean" we show the mean of all members (if at least 4 members project into a regime) for surface variables such as 2m temperature, 2m temperature anomaly, 100m wind speed, 100m wind speed anomaly, 6h precipitation and total cloud cover. This shows the differences in surface weather for the current configuration of a regime. For our example the ScBL scenario would be cold, whereas the AT scenario would bring mild conditions into Europe (**Figure 7**).

Finally, the plot **"WR Index ana"** shows the weather regime index I_{wr} computed for the unfiltered analysis during the last 30/90/365 days. The maximum index I_{wr} is highlighted in bold, if it is above 1.0. Here we only show the sub-panel for the last 30 days back from 28 January 2019 (**Figure 8**).

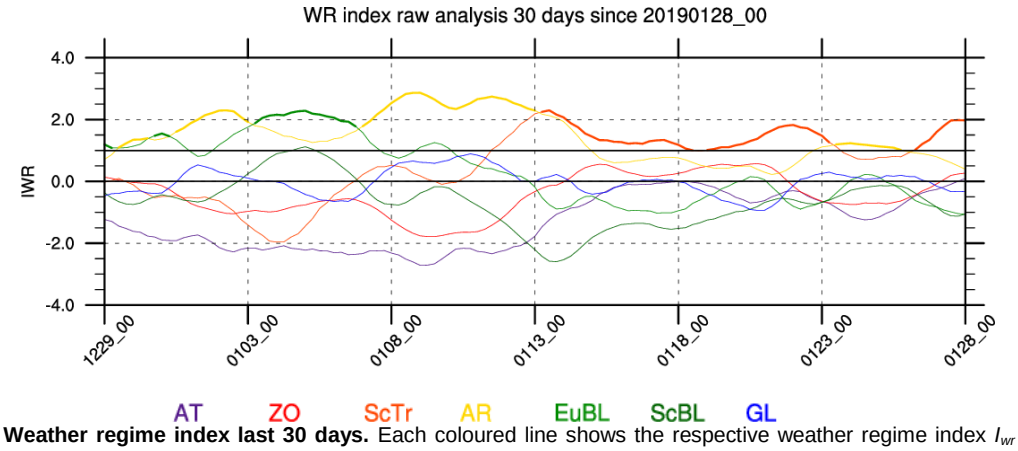

Figure 8: Weather regime index last 30 days. Each coloured line shows the respective weather regime index I_{wr} based on unfiltered analysis data for the 30 days ending at 00 UTC 30 January 2019. Period where the maximum I_{wr} > 1.0 are highlighted in bold. Legend indicates colour coding.

Extended-range ensemble (0-45 days)

For the bi-weekly (Mondays and Thursdays) extended-range ensemble forecasts we provide the key figures **"Weather Regimes", "WR Members"**, and **"WR Index"**, as well as the simplified overviews **"WR Simple LC"** and **"WR maxIWR"**. Note that the raw extended-range forecast is identical to the medium-range forecast for the first 15 days. For the extended-range regime attribution in "Weather Regimes" and "WR Members", however, we use the original weather regime life cycle definition of Grams et al. (2017) based on 5 day low-pass filtered Z500 anomalies and a sophisticated life cycle definition that requires 5 day persistence and allows merging of neighbouring life cycles (see Section 3). In the example forecast initialisation time of 00 UTC 28 January 2019, the stricter persistence hinders the detection of an active ScTr life cycles early in the forecast (cf. **Figure 3** and **Figure 9**). We show "WR Members" and "WR Index" without further discussion (**Figure 10,11** cf. **Figures 4,5**).

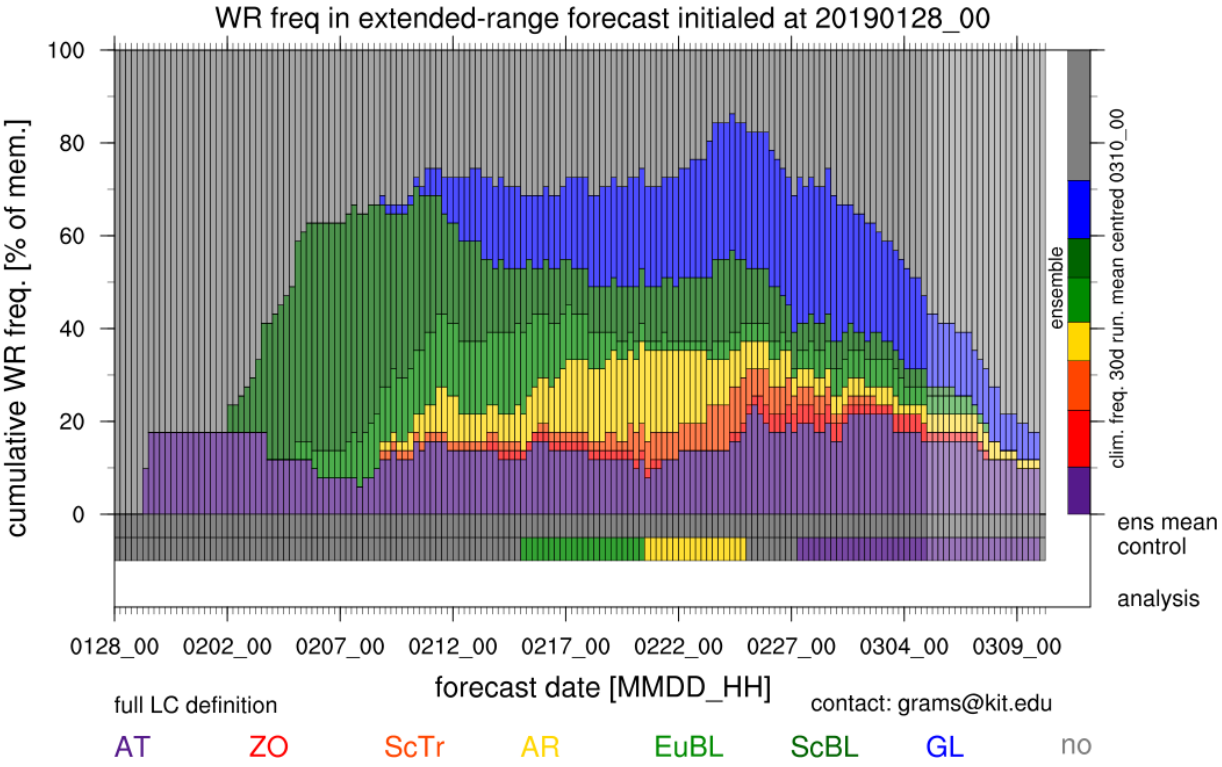

Figure 9: "Weather regimes" plot for the extended-range. Example for ECMWF IFS ensemble initialised at 00 UTC 28 January 2019. Stacked bars show the relative number of members projecting in one of the 7 weather regimes or no regime following the full weather regime life cycle definition of Grams et al. (2017). The bottom rows show the attribution of the ensemble mean and control forecasts, respectively. The last 120h are shown in pale colours as the persistence criterion is systematically less likely meet (see Section 3). Note that the forecast is only shown up to 40 days as the last 5 forecast days are cut due to Lanczos filtering.

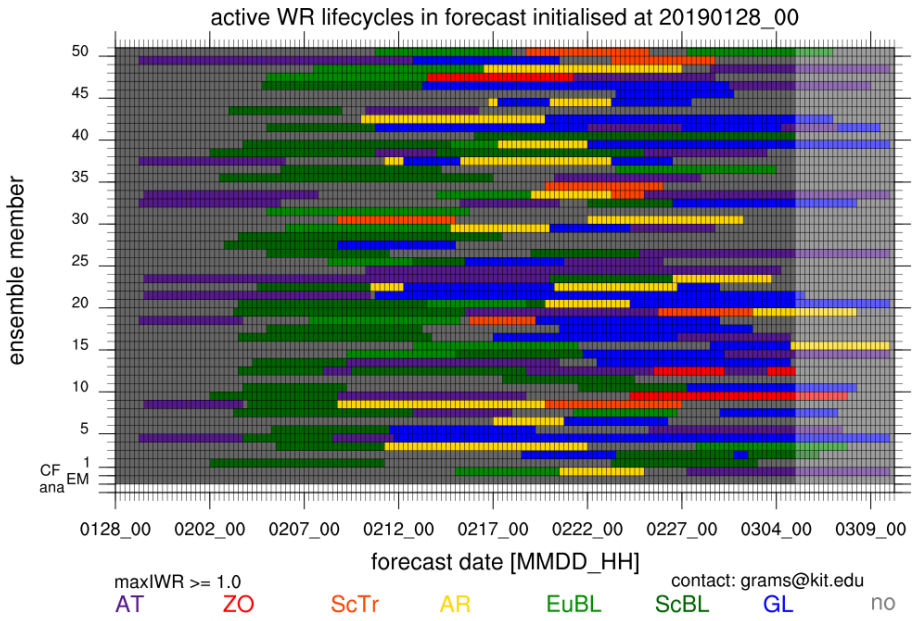

Figure 10: "WR Members" plot. Currently active weather regime life cycles for the extended-range forecast and each member and at each forecast step. The last 120h are shown in pale colours as the persistence criterion is systematically less likely meet (see Section 3).

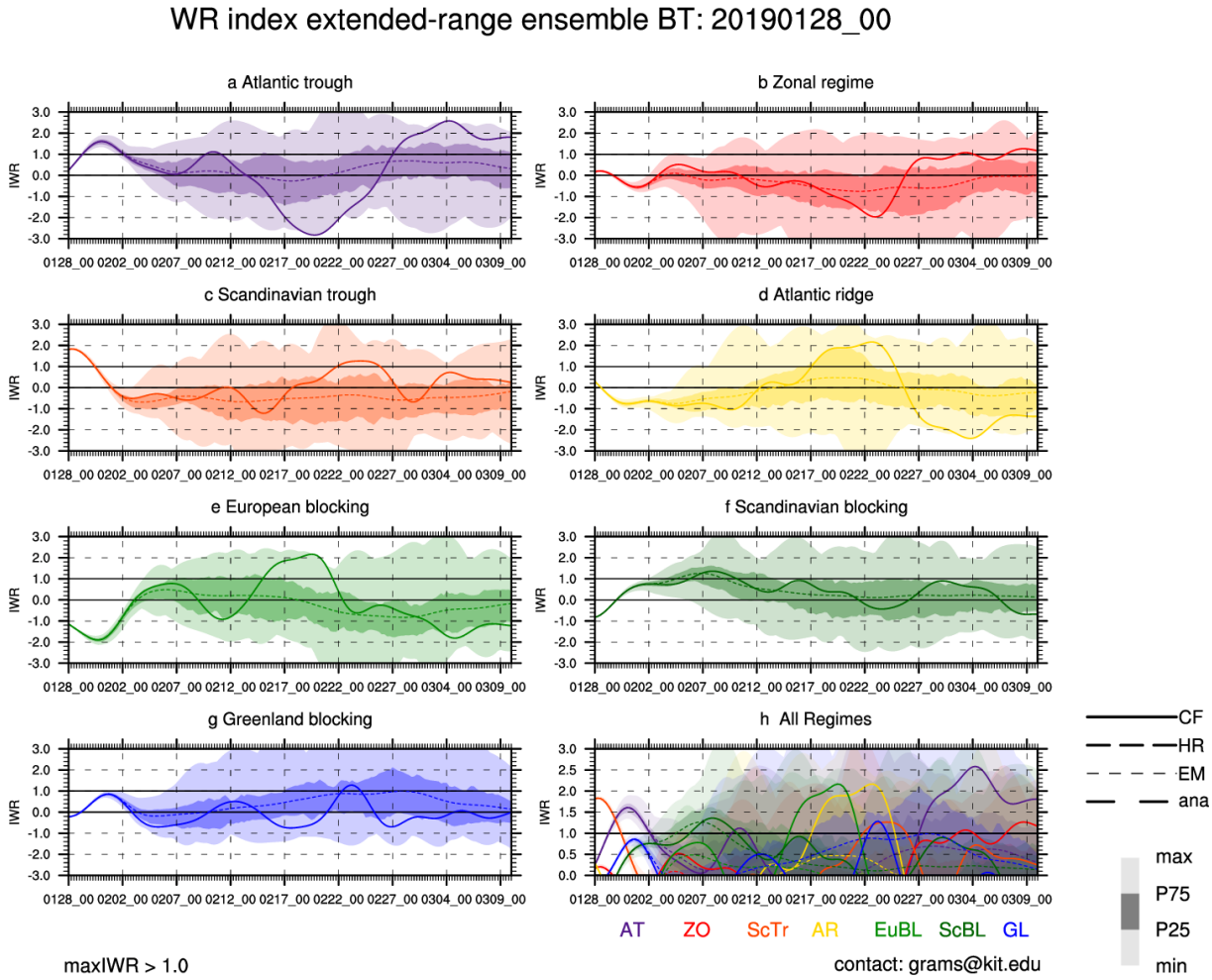

Figure 11: "WR index" plot for the extended-range. Panels a-g show the distribution of the respective weather regime index I_{wr} at each forecast step. Light shades show the bounds given by the members with the maximum and minimum projection, dark shades show the 75th and 25th percentile. Lines show the projection of the control forecast (bold solid) and ensemble mean (thin dashed). The last panel h compares all projections by zooming only on positive values.

3. Technical Implementation

Weather regime definition

The Atlantic-European weather regime definition is based on standard approaches using empirical orthogonal function analysis (EOF) and k-means clustering (Michelangeli et al. 1995; Michel and Rivière 2011; Ferranti et al. 2015). EOF analysis is performed on the 10-day low-pass filtered geopotential height anomaly (using a 90-day running mean at the respective calendar time as reference climatology) at 500 hPa (*Z500'*) in the domain 80°W to 40°E, 30°N to 90°N. Global data from ERA-Interim (Dee et al. 2011) at 1° horizontal resolution are used six-hourly from 11.01.1979 to 31.12.2015. We use ERA-Interim for the weather regime definition, as this reanalysis is thought to feature the best depiction of the large-scale circulation. The seasonal cycle in the amplitude of the anomaly is removed prior to the EOF clustering by computing at each grid point the temporal standard deviation in a running 30-day window for each calendar time, and normalising *Z500'* by the spatial mean of this running standard deviation in the EOF domain. The leading seven EOFs (76.7% of explained variance) are used for the k-means clustering, which is repeated 10 times to test convergence to a stable solution. The optimal number of clusters is seven based on the criterion that the anomaly correlation coefficient (ACC) between the clusters is below 0.4. This number of regimes is larger than the 4 weather regimes commonly used in previous studies and found to be optimal by various authors (cf. Michelangeli et al. 1995; Michel and Rivière 2011; Ferranti et al. 2015) albeit when considering only a specific season, mostly winter. As explained for instance in the Supplement of (Cassou 2008), Atlantic-European weather regimes have a strong seasonal cycle and are most distinct between winter and summer, with an optimal number of 4 clusters in each season. A novel aspect of our classification is that it allows identifying regimes year-round. These regimes are the winter and summer patterns described in the literature. The GL regime is similar in all seasons, explaining why we find just 7 rather than 8 year-round regimes. The seasonal preference for each regime is reflected in the monthly frequencies (**Figure 2**), but each of the 7 flow patterns can occur in all seasons. The objective weather regime index (Michel and Rivière 2011) I_{wr}, using the projection of the instantaneous *Z500'* to the cluster mean, is computed to derive individual weather regime life cycles. To derive objective weather regime life cycles in the ERA-Interim period and compute composite anomalies for various fields **(**see **Appendix 1** and **Appendix 2)** time steps from 10.01.1979 to 30.06.2016 are attributed to a weather regime life cycle if $I_{wr} > 1.0$, the period of $I_{wr} > 1.0$ lasts for at least 5 days, and it contains a local maximum with a monotonic increase/decrease of I_{wr} during the previous/following 5 days. Here *wr* are *wr* = AT, ZO, ScTr, AR, EuBL, ScBL, GL. Subsequent life cycles of the same weather regime are merged if the mean I_{wr} during the duration of the joint life cycle is larger than the threshold 1.0. If the projection I_{wr} to more than one regime fulfils these criteria, the respective calendar time is attributed to the regime with maximum I_{wr}. This full life cycle definition is also applied to **extended-range ensemble** forecast data but using a 5-day low-pass filter to reduce the data cut-off at the end of the forecast. For time steps prior to initial time analysis data is used to apply the full life cycle definition which considers periods of at least 5 days test persistence for an individual time step. For the **medium-range** we use an alternate definition requiring only that $I_{wr} > 1.0$ for at least 4 days as described below.

Attribution of ensemble forecast members to weather regimes

To attribute each of the 50 ECMWF IFS **medium-range** ensemble members, the ensemble control forecast (CF), the ensemble mean (EM), and high resolution forecast (HRES) to one of the seven regimes we compute I_{wr} for each of them. However, here we use raw data, i.e. we do not apply the low-pass filter.

First *Z500'* is computed with respect to the ERA-Interim 90 day running mean *Z500* at forecast initialisation time for each ensemble member and each six-hourly forecast time (0-360h, only 0-240h for HRES). Then this instantaneous *Z500'* is normalised using the weight as for the weather regime definition valid for the respective calendar time. We then compute I_{wr} for these normalised anomalies as the anomaly of the projection into the mean anomaly of the respective regime, normalised by the standard deviation of the projection (Michel and Rivière 2011).

Based on I_{wr} the attribution of each member at each forecast time a member to a weather regime is computed as follows. First we identify the maximum I_{wr} (shown in plot "WR maxIWR"). Second, we check if $I_{wr.}$ is above a threshold of 1.0. If this is not fulfilled we attribute the respective time step and member to "no regime". This instantaneous attribution is shown in plot "WR SimpleLC". Finally, we check if the maximum I_{wr} occurs within a period of at least 96h with I_{wr} >1.0 (not necessarily maximum at each time step in that period). The latter attribution method includes persistence and is used to construct the main plots "Weather regimes", "WR Members" and the composites of Z500 and of surface variables.

NAO index

To analyse the correspondence between the weather regimes and the NAO, we use the daily NAO index of the Climate Prediction Center (CPC) at NOAA, http://www.cpc.noaa.gov/products/precip/CWlink/pna/nao.shtml retrieved on 6 December 2016), based on a rotated EOF analysis of normalised 500 hPa geopotential height anomalies (Barnston and Livezey 1987). Note that this NAO definition uses the seasonal varying patterns of the first EOF valid for each calendar month, and weighted for the considered day. In contrast, our weather regime definition uses a constant EOF pattern year-round, based on the leading 7 EOFs. In our data, these 7 EOFs explain 76.7% of the variance in *Z500',* whereas the first EOF, which represents the NAO, only explains 19.6%. The mean NAO indices for all days in one of the weather regimes are given in **Table 1**.

Appendix 1: Modulation of surface weather

The weather regimes are accompanied by important changes in near surface weather conditions. These modulations are different in different seasons. Here we present the seasonal anomalies of variables for each of the regimes without further discussion. The variables are: *Z500*, 2m temperature, precipitation, 100m wind speed (for wind power applications), and the fraction of maximum potential insolation (for solar power applications). These figures help interpreting which surface conditions one might expect if a specific regime is active. However, note that there is also intra-regime variability and therefore these anomalies reflect expected mean surface weather for the entire period when a regime is active (usually several days), but not for an instantaneous forecast time step.

Winter anomalies

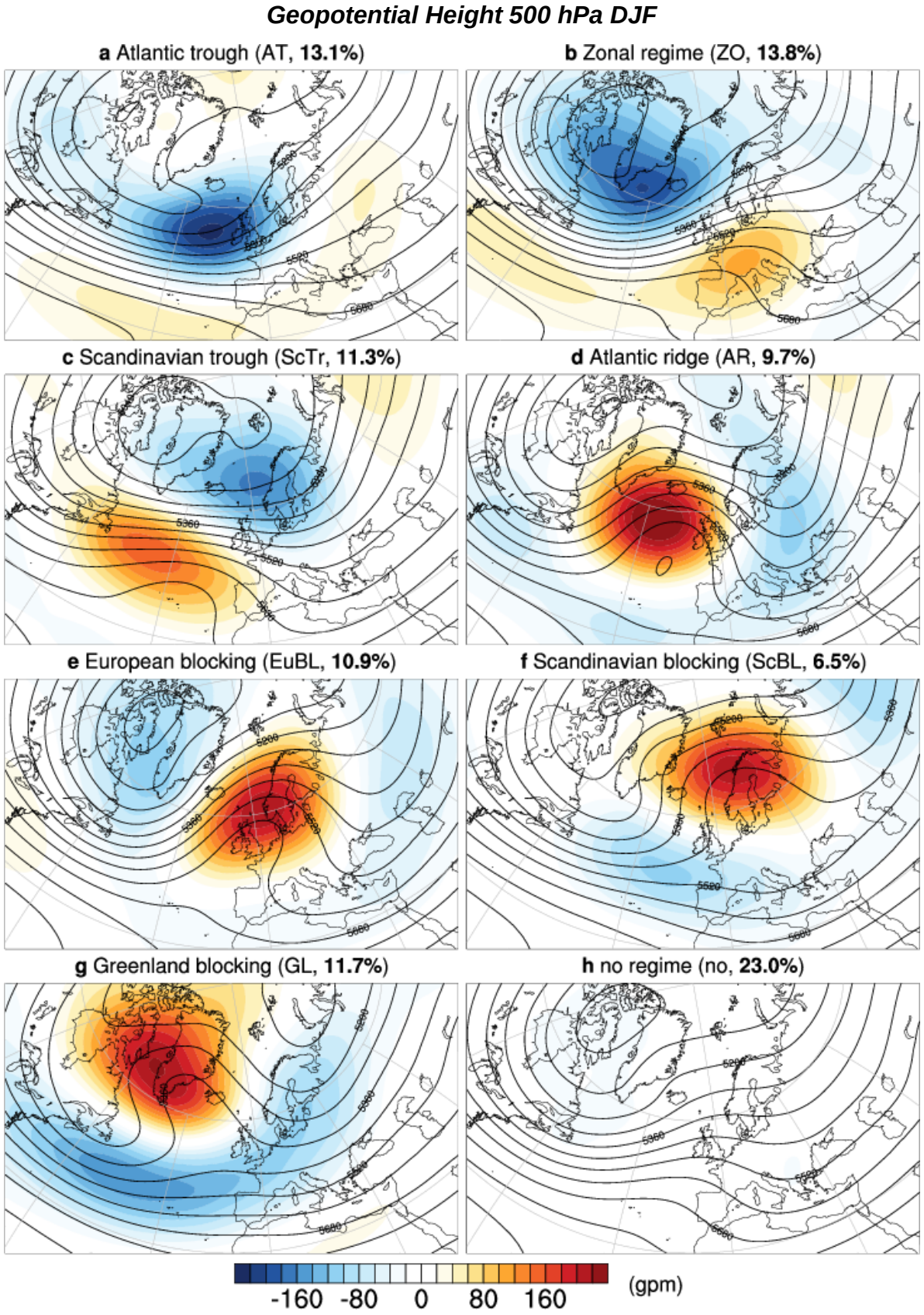

Figure 12: Atlantic European weather regimes in winter (DJF). As **Figure 1** but for winter. Mean low-pass filtered (10 days) 500 hPa geopotential height anomaly (Z500', shading, every 20 geopotential meters), and mean absolute 500 hPa geopotential height (Z500, black contours, every 40 geopotential meters) for all winter days (DJF) in ERA-Interim (1979-2015) attributed to one of the 7 weather regimes (a-g) and to no regime (h). Although the regime definition is based on normalised data, here non-normalised data are shown. Regime name, abbreviation, and relative frequency (all winter in percent) indicated in the sub-figure caption.

100m Wind DJF

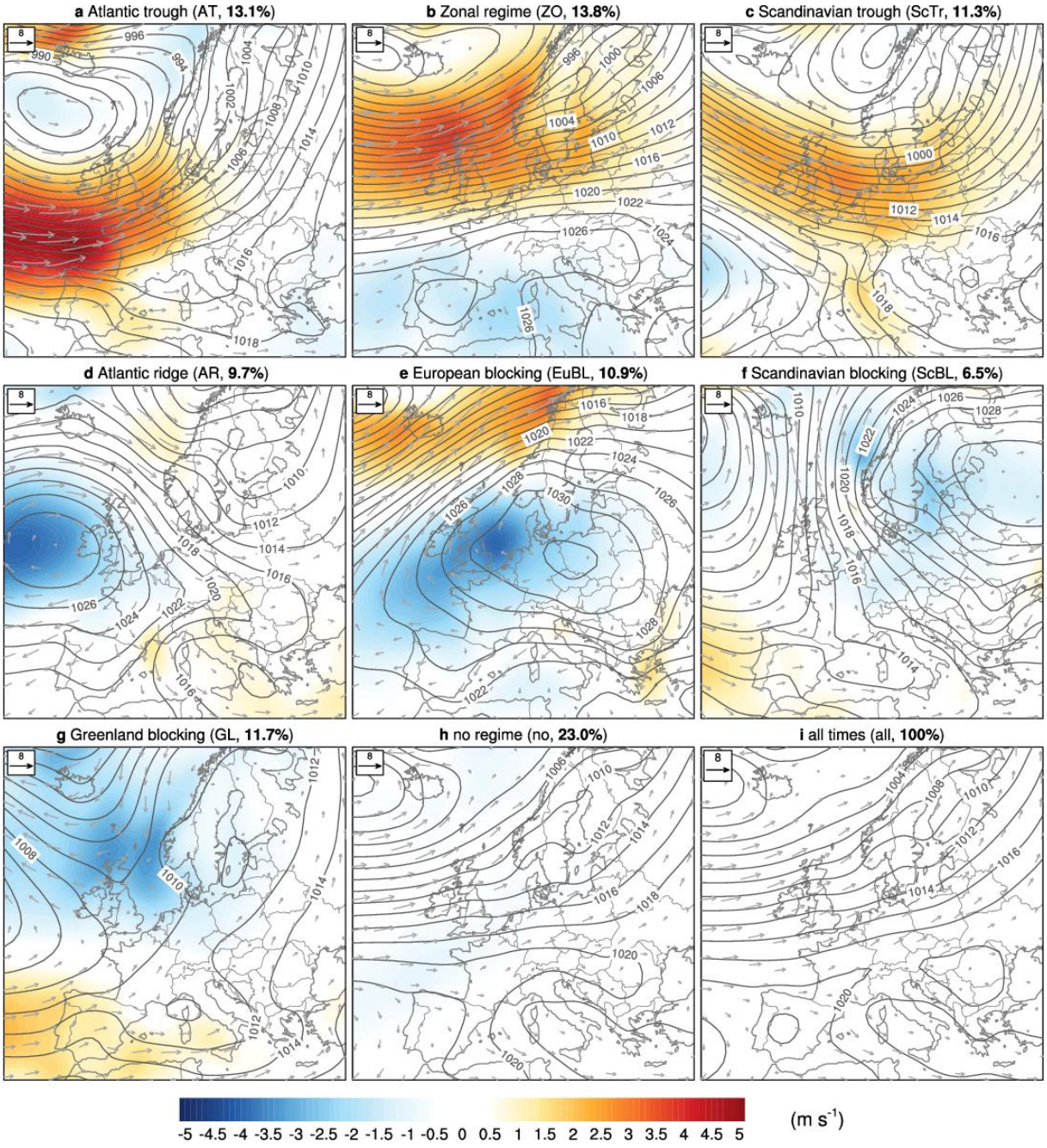

Figure 13: Wind anomalies during the weather regimes in winter (DJF). 100 m wind speed anomalies (blue-red shading in m s-1), absolute wind at about 100 m (grey vectors), and mean sea level pressure (contours every 2 hPa) for all winter days (DJF) in ERA-Interim (1979-2015) during each regime (a-g), no regime (h), and whole winter (i).

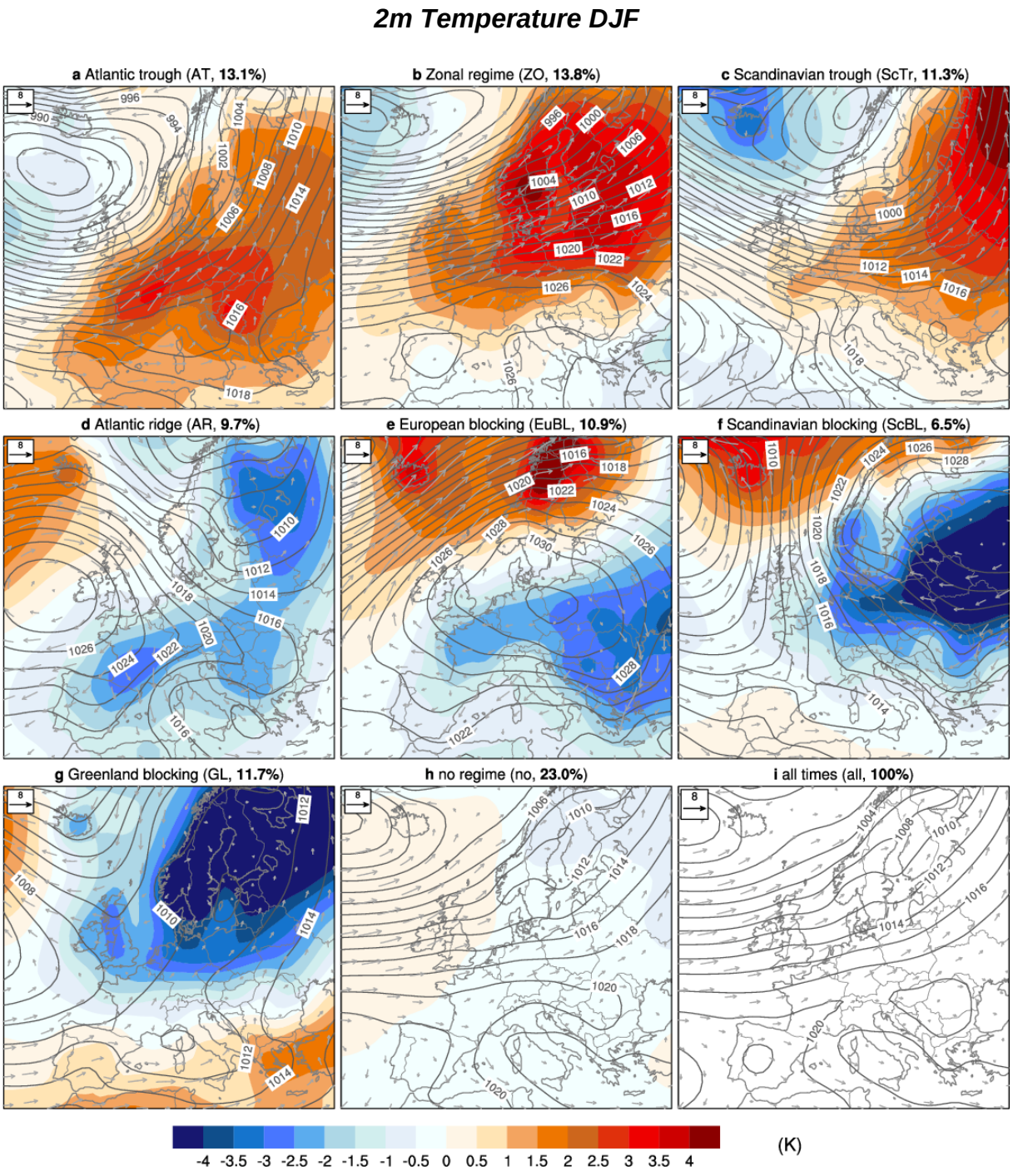

Figure 14: 2m temperature anomalies during the different weather regimes in winter (DJF). Anomalies of 2 m temperatures (blue-red shading in K) computed with respect to the 30-day running average at the respective calendar day, absolute wind at about 100 m (grey vectors), and mean sea level pressure (contours every 2 hPa) for all winter days (DJF) in ERA-Interim (1979-2015) during each regime (a-g), no regime (h), and whole winter (i).

Precipitation DJF

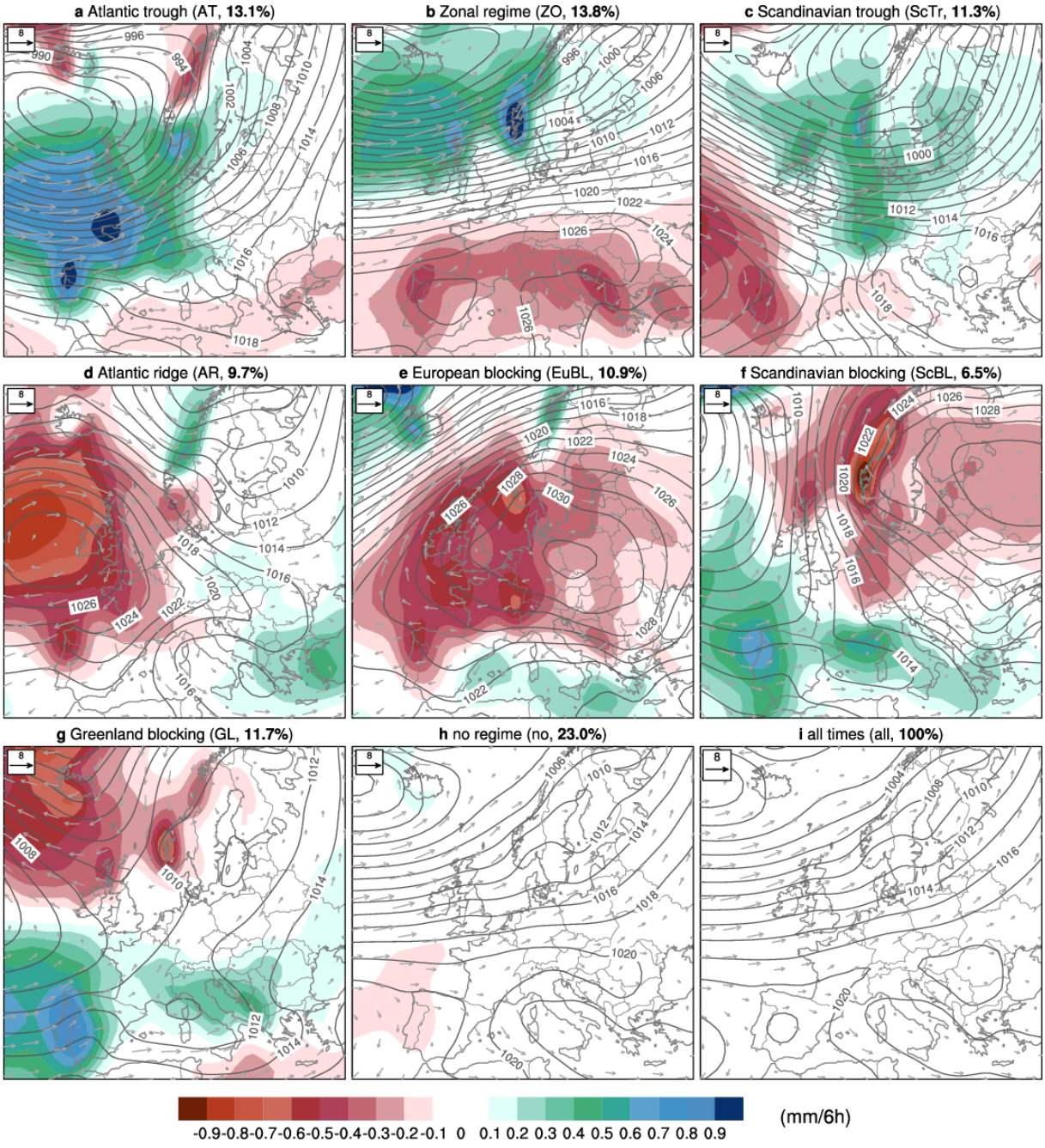

Figure 15: Precipitation anomalies during the different weather regimes in winter (DJF). Anomalies of six-hourly precipitation (red-blue shading in mm $(6h)^{-1}$) computed with respect the winter mean, absolute wind at about 100 m (grey vectors), and mean sea level pressure (contours every 2 hPa) for all winter days (DJF) in ERA-Interim (1979-2015) during each regime (a-g), no regime (h), and whole winter (i).

Fraction of possible Insolation DJF

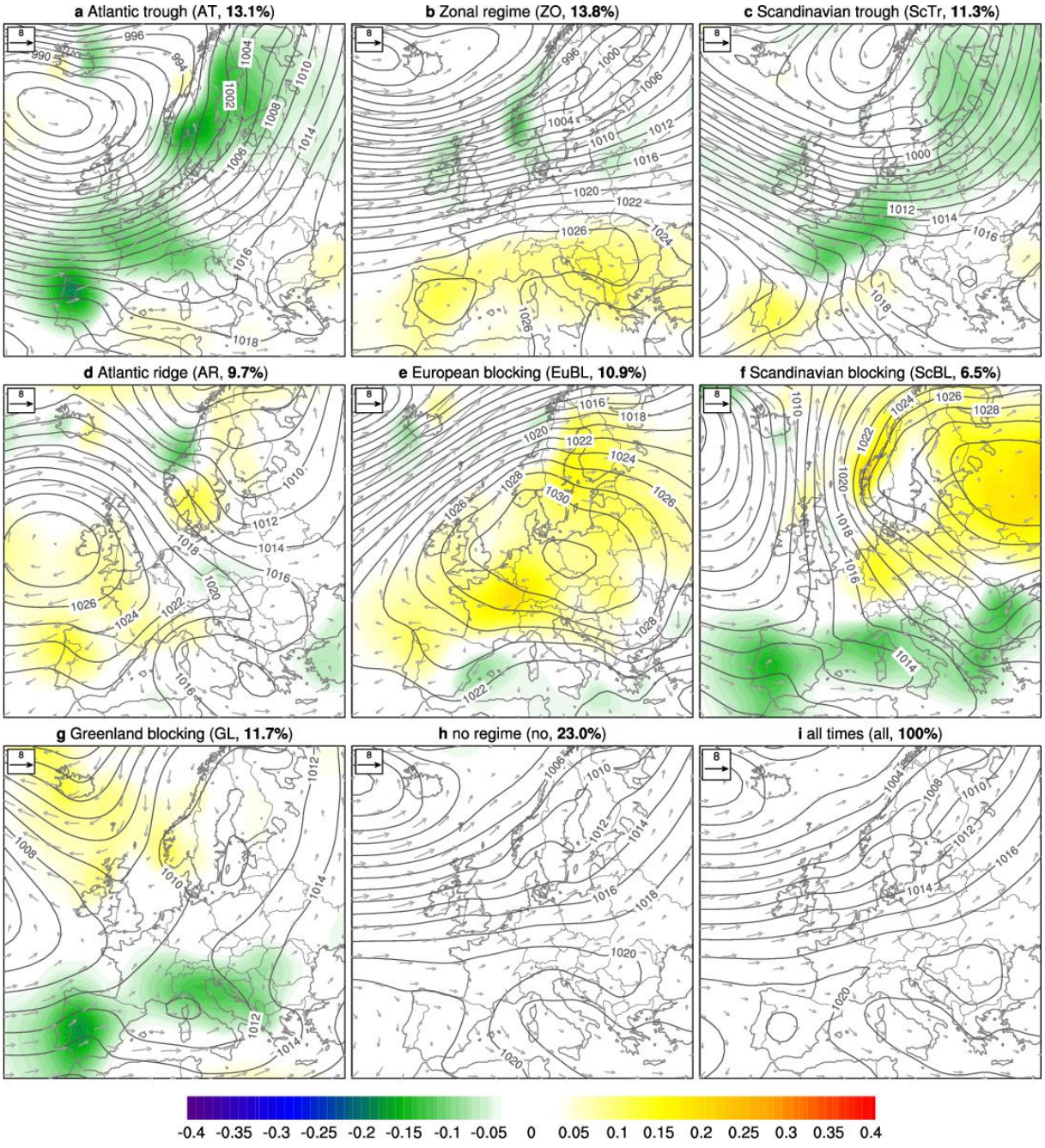

Figure 16: Insolation anomalies during the different weather regimes in winter (DJF). Anomalies of the daily fraction of insolation and daily potential insolation assuming clear skies (green-yellow shading), absolute wind at about 100 m (grey vectors), and mean sea level pressure (contours every 2 hPa) for all winter days (DJF) in ERA-Interim (1979-2015) during each regime (a-g), no regime (h), and whole winter (i).

Spring anomalies

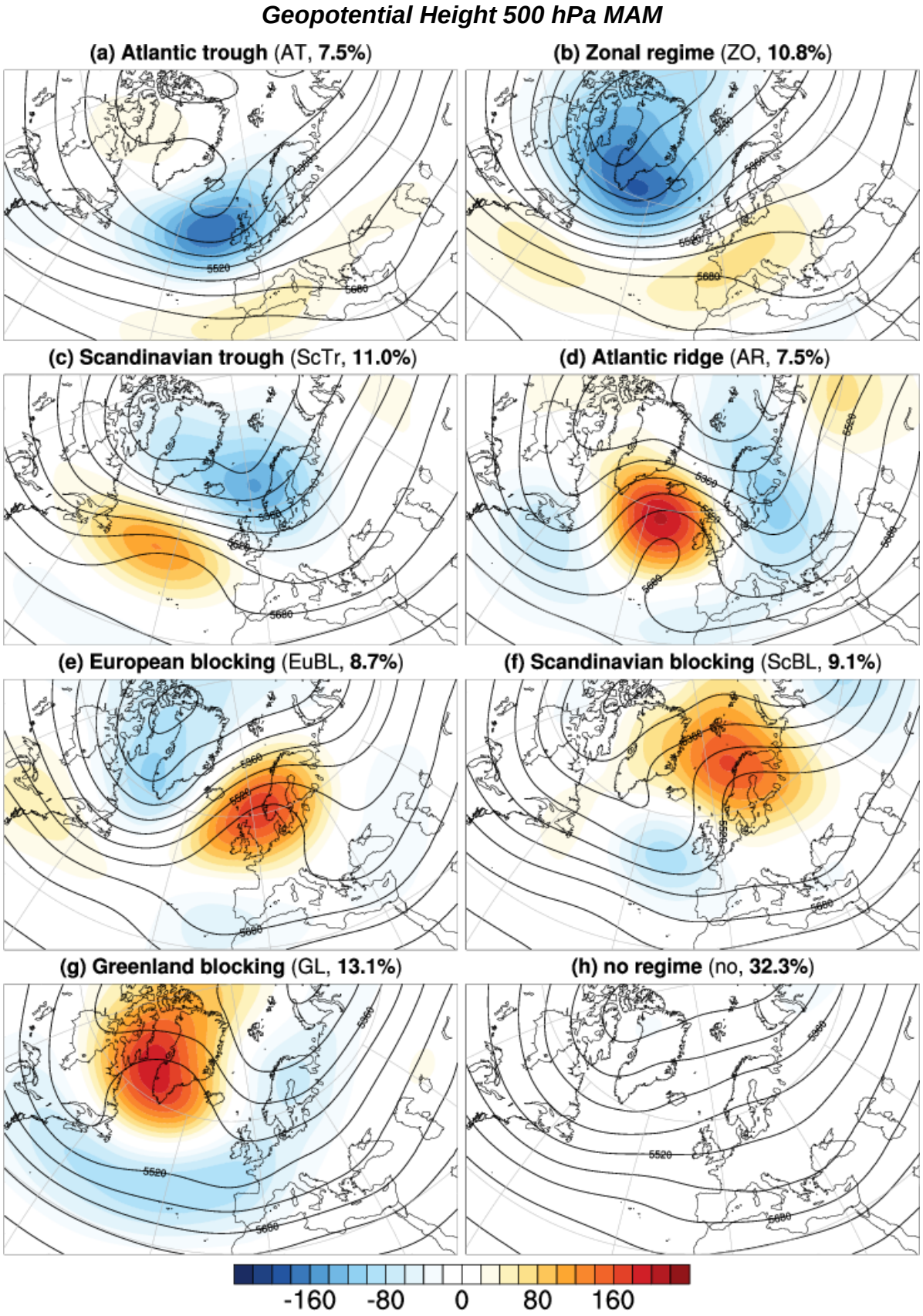

Figure 17: Atlantic European weather regimes in spring (MAM). As **Figure 12** but for spring (MAM).

100m Wind MAM

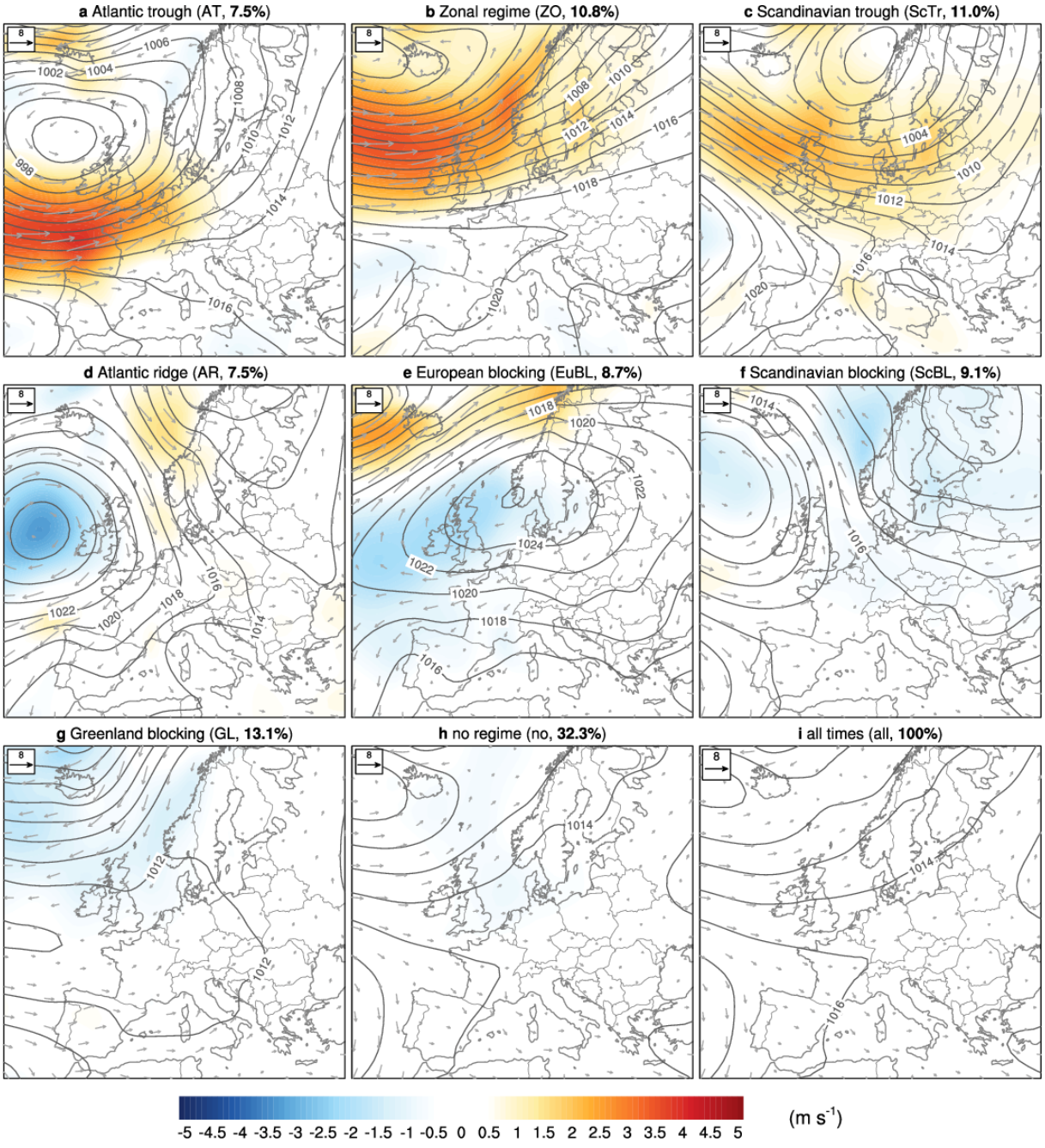

Figure 18: Wind anomalies during the weather regimes in spring (MAM). As

Figure 13 but for spring (MAM).

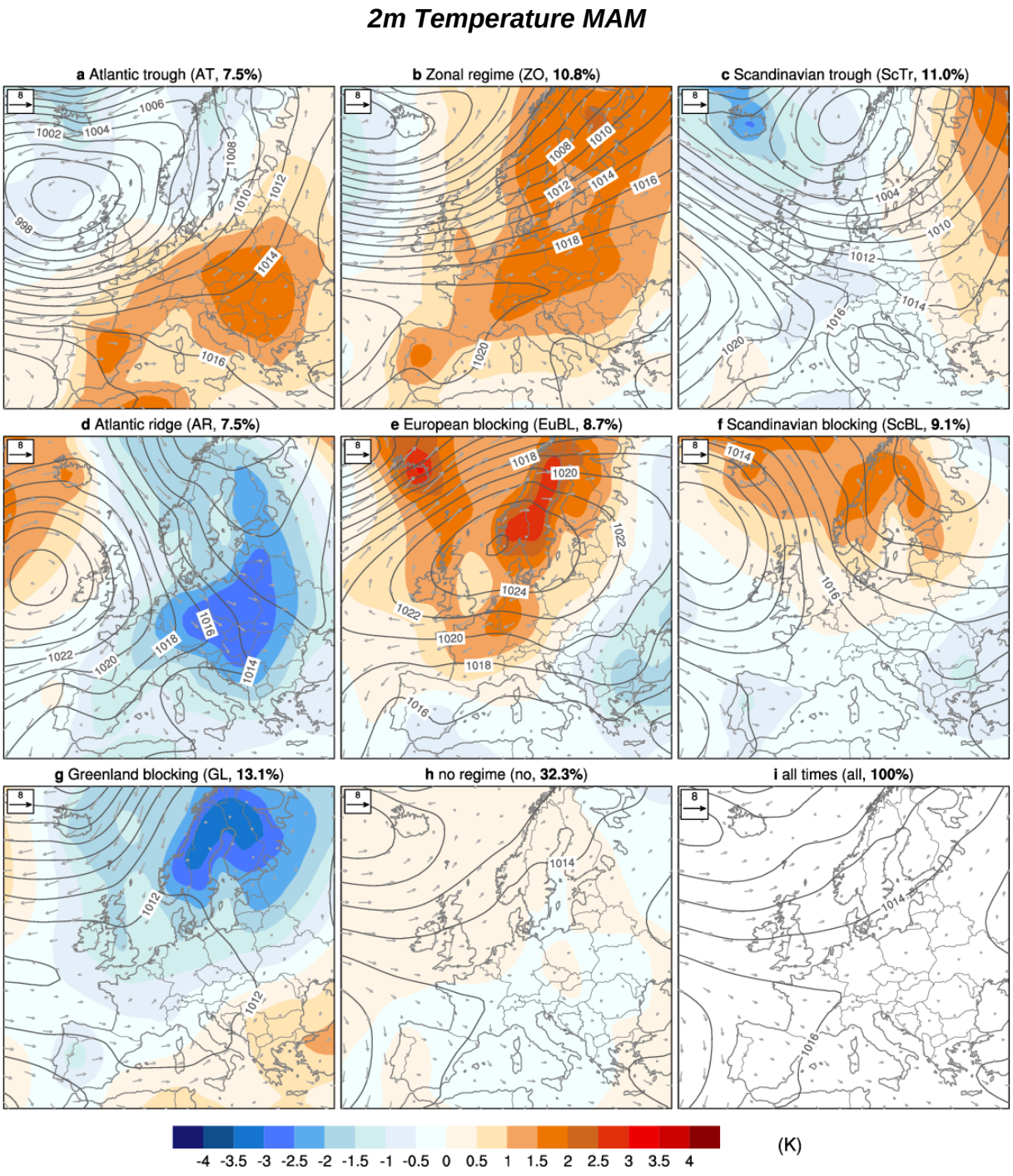

Figure 19: 2m temperature anomalies during the different weather regimes in spring (MAM). As **Figure 14** but for spring (MAM).

Precipitation MAM

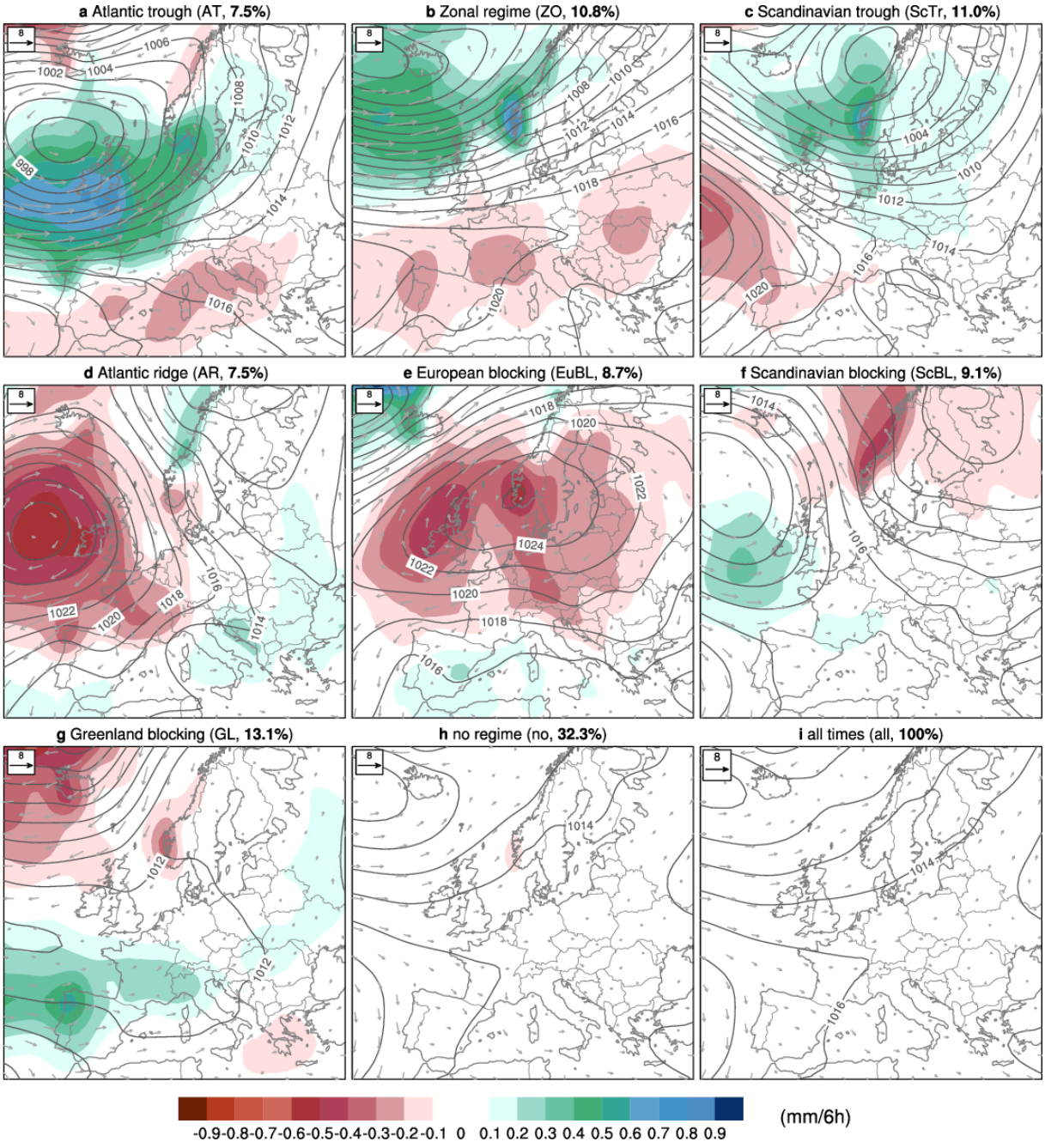

Figure 20: Precipitation anomalies during the different weather regimes in spring (MAM). As **Figure 15** but for spring (MAM).

Fraction of possible Insolation MAM

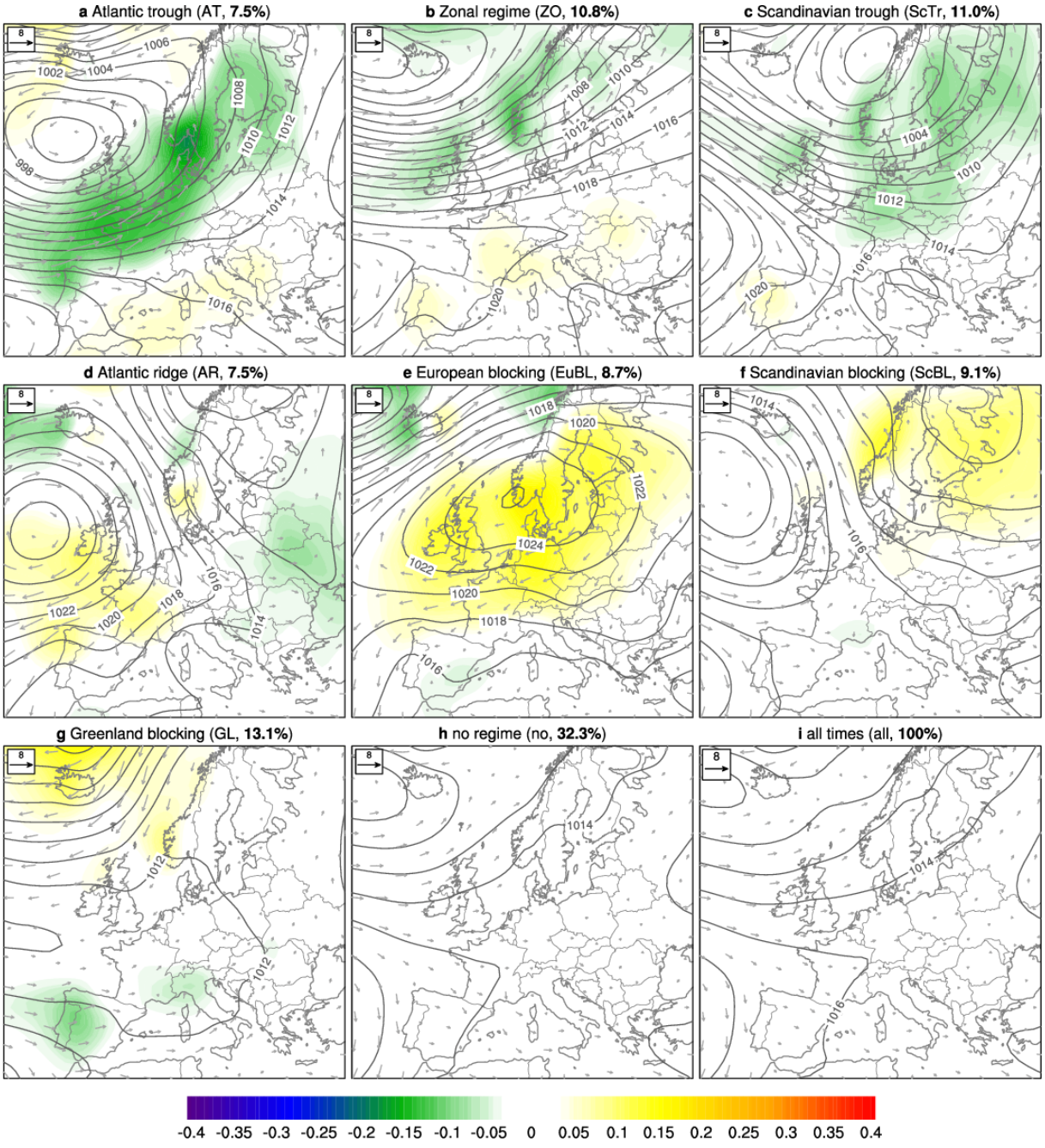

Figure 21: Insolation anomalies during the different weather regimes in spring (MAM). As

Figure 16 but for spring (MAM).

Summer anomalies

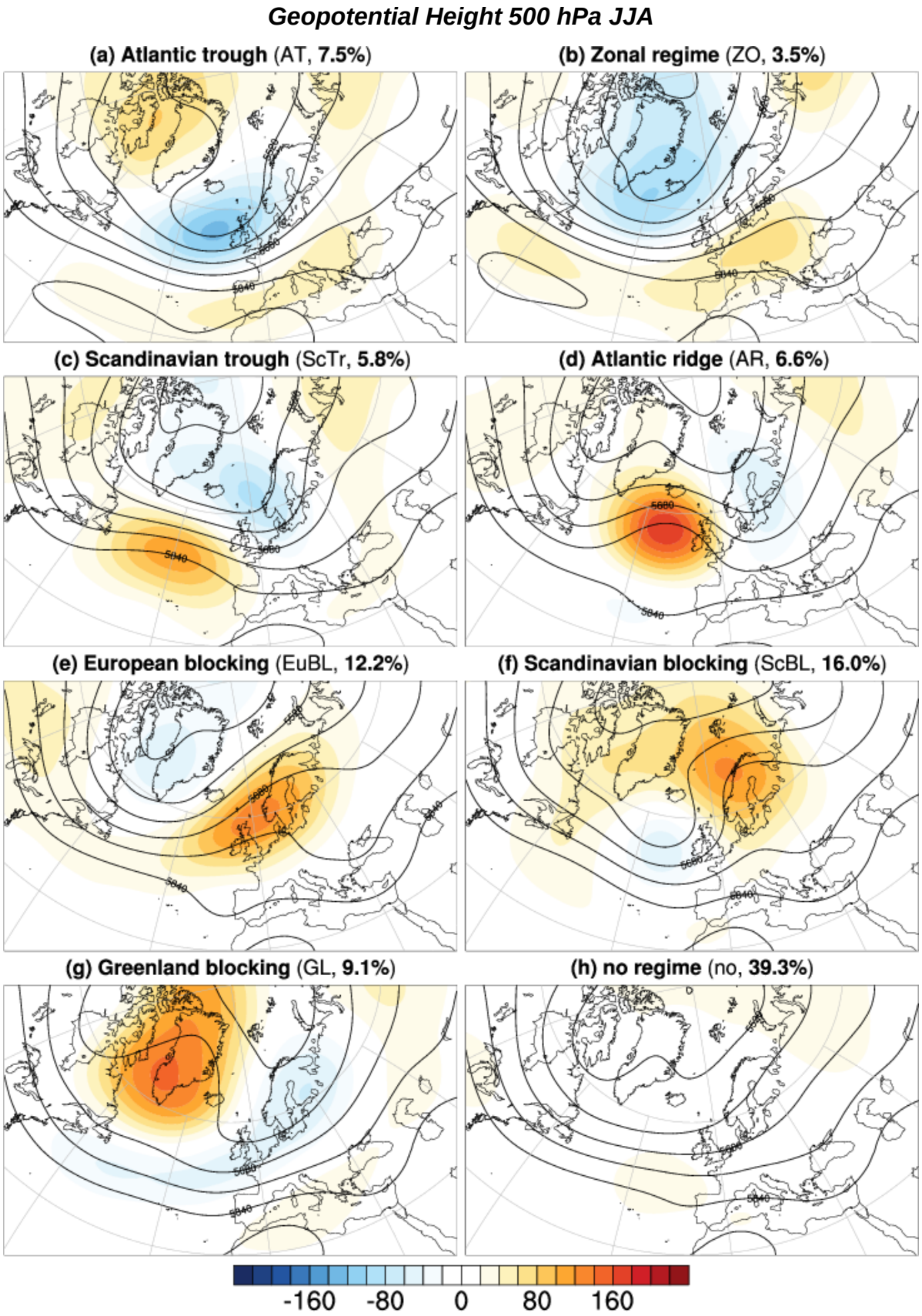

Figure 22: Atlantic European weather regimes in summer (JJA). As **Figure 12** but for summer (JJA).

100m Wind JJA

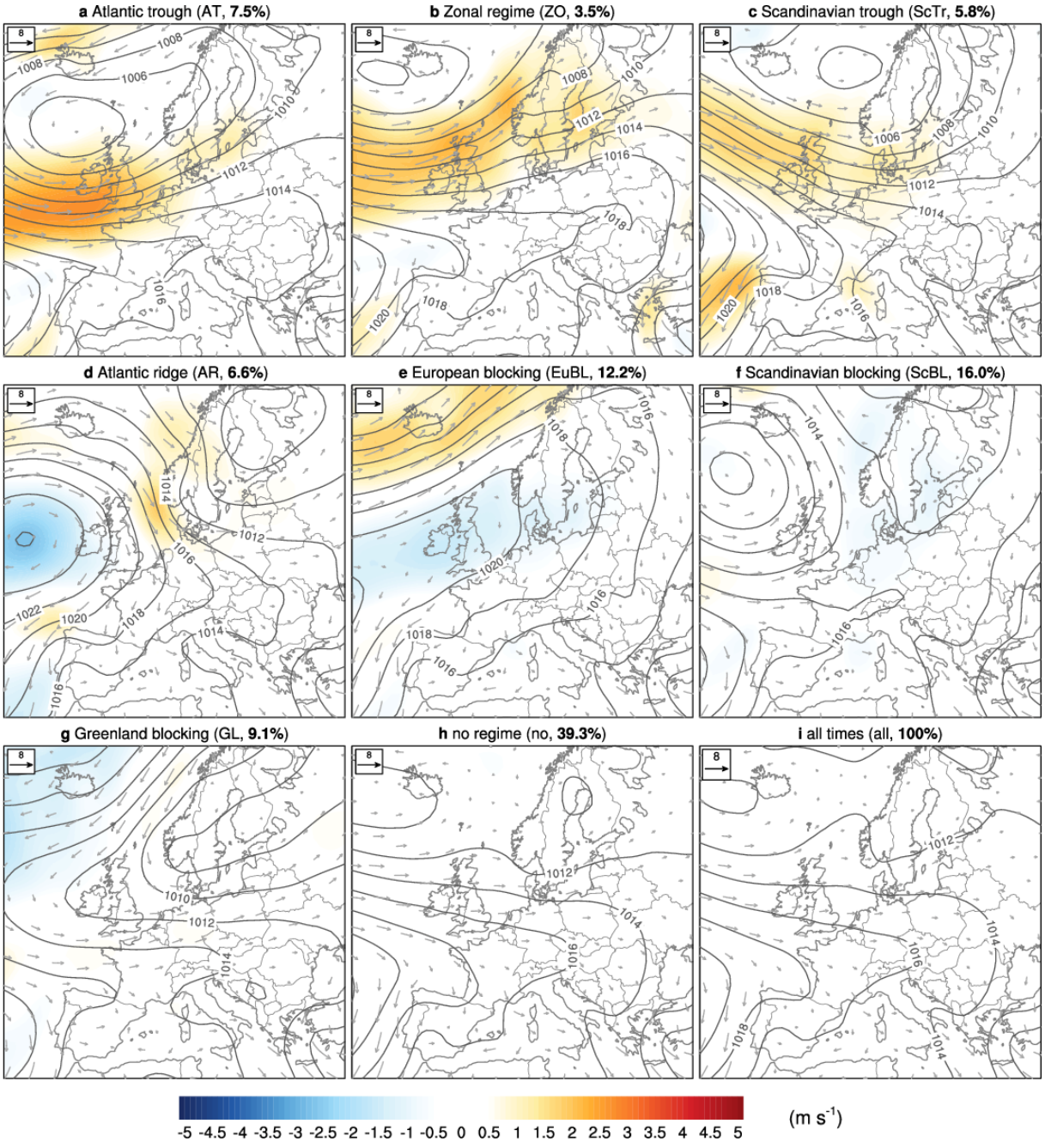

Figure 23: Wind anomalies during the weather regimes in summer (JJA). As

Figure 13 but for summer (JJA).

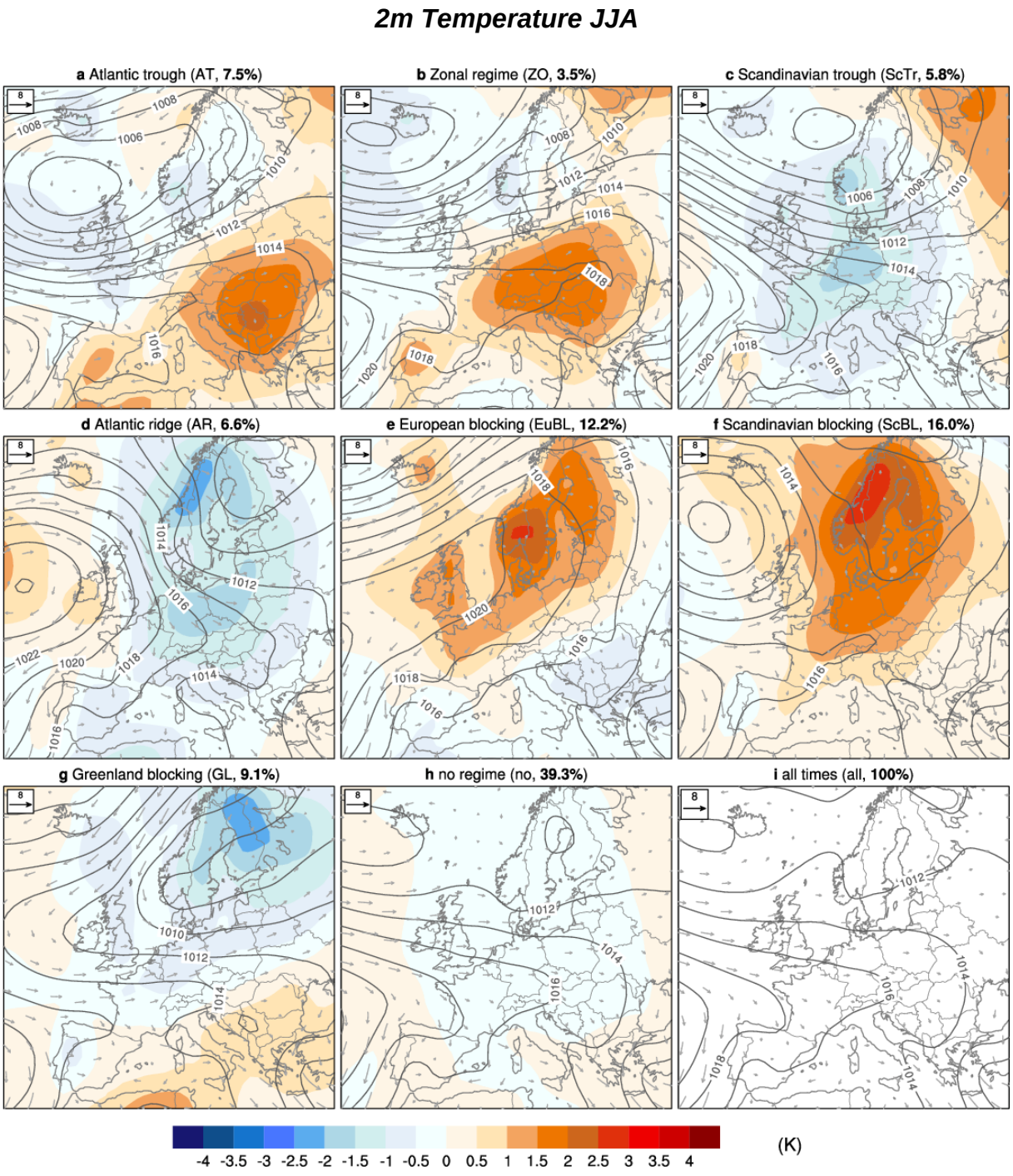

Figure 24: 2m temperature anomalies during the different weather regimes in summer (JJA). As **Figure 14** but for summer (JJA).

Precipitation JJA

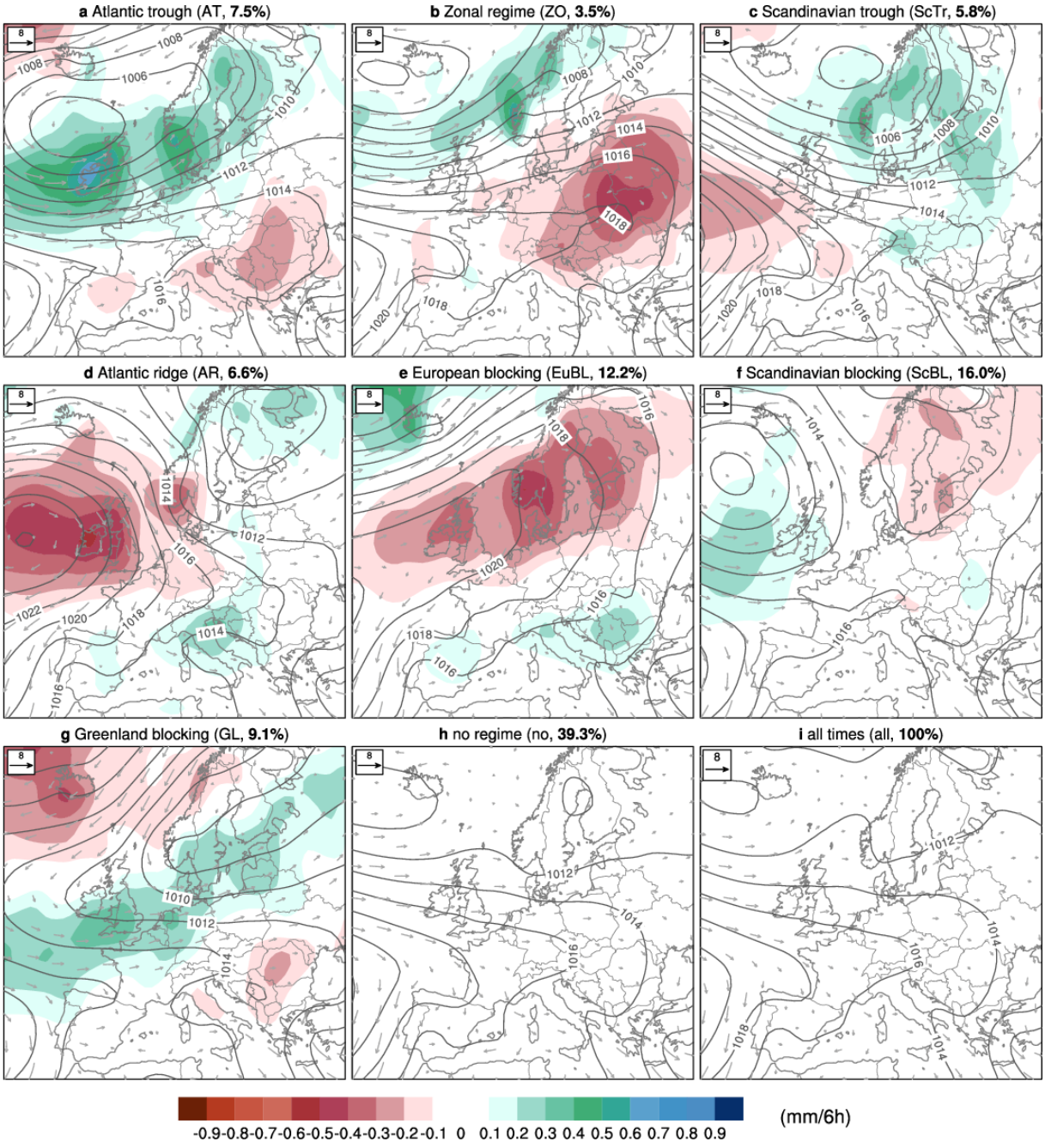

Figure 25: Precipitation anomalies during the different weather regimes in summer (JJA). As

Figure 15 but for summer (JJA).

Fraction of possible Insolation JJA

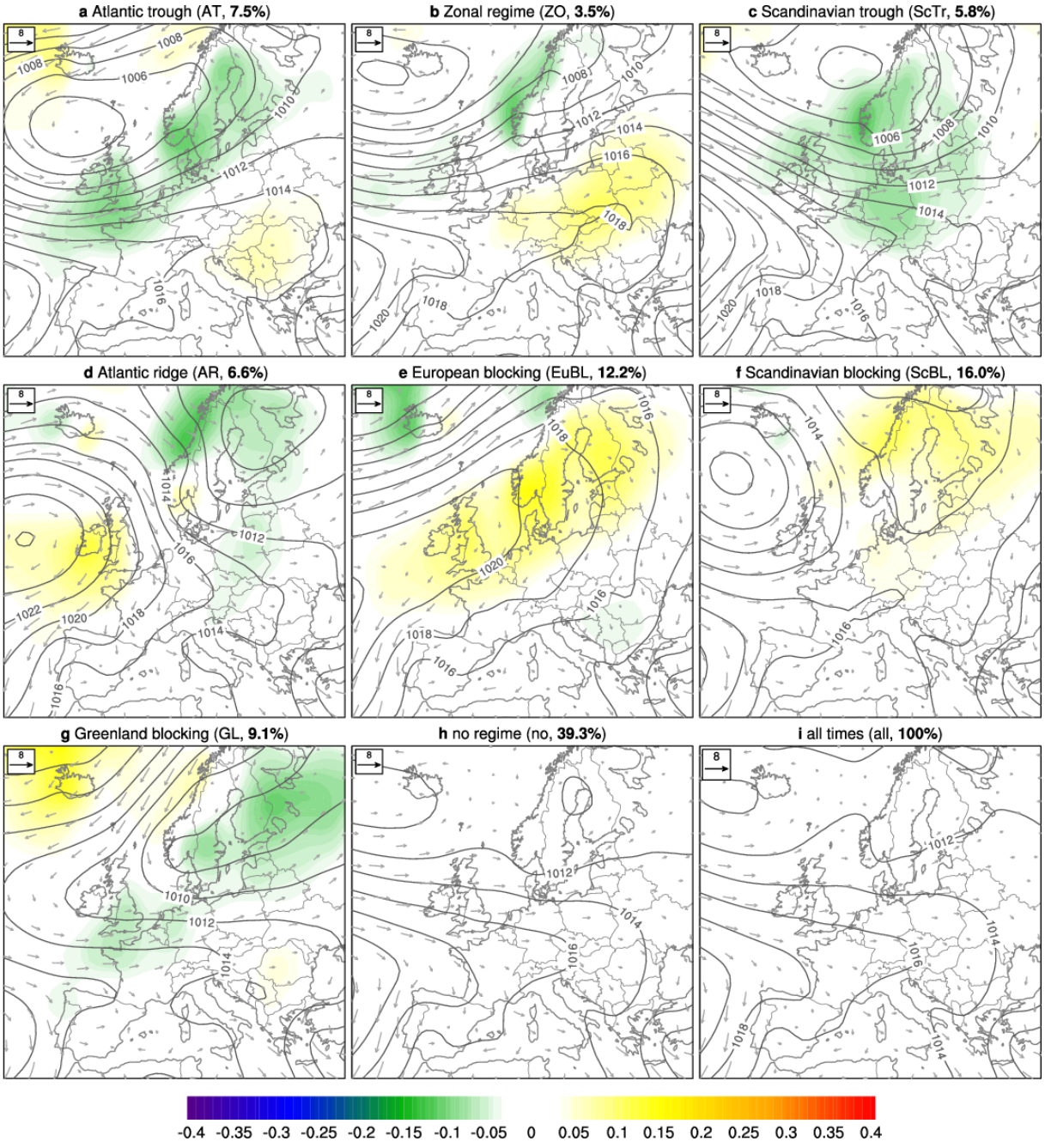

Figure 26: Insolation anomalies during the different weather regimes in summer (JJA). As

Figure 16 but for summer (JJA).

Autumn anomalies

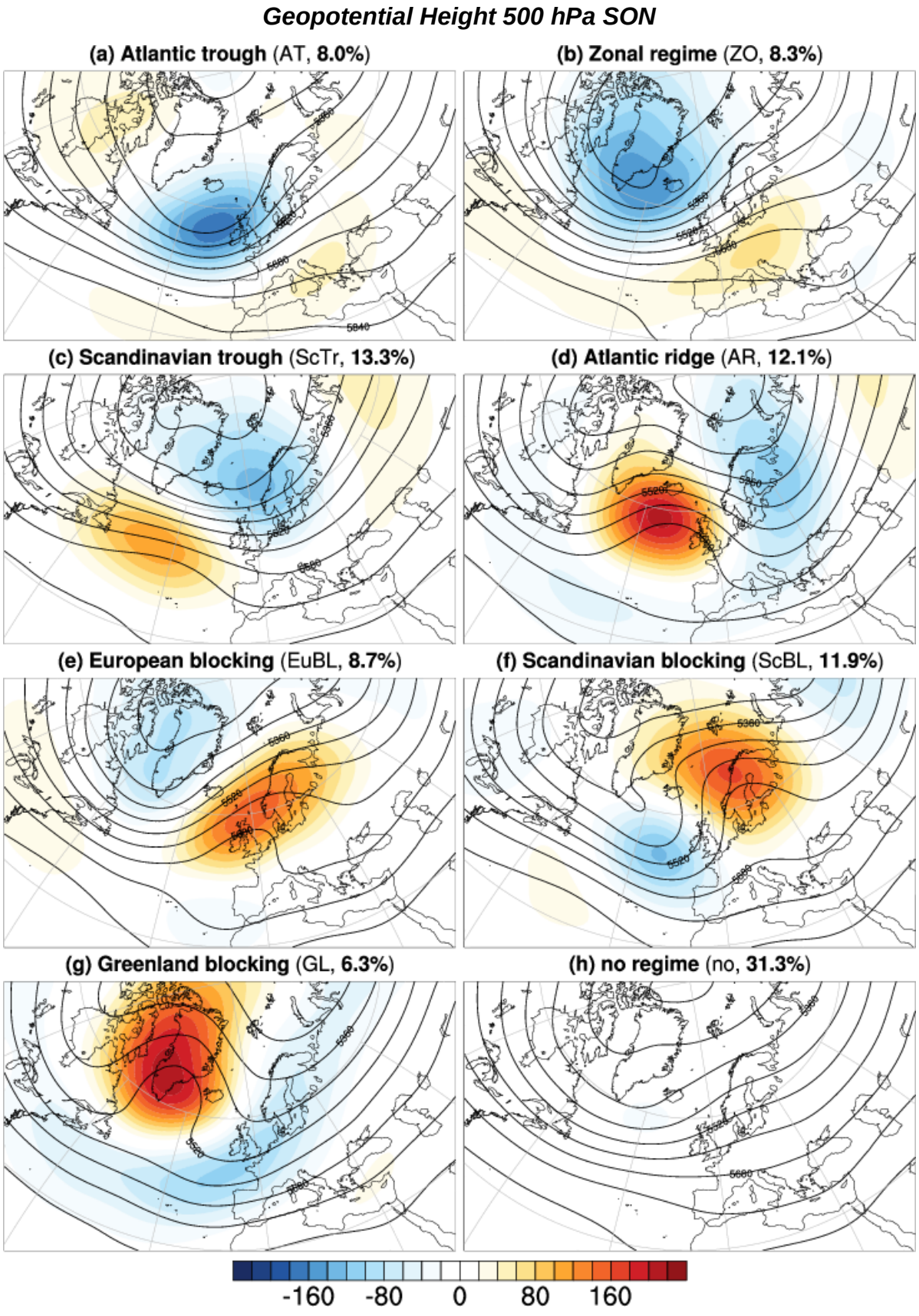

Figure 27: Atlantic European weather regimes in autumn (SON). As **Figure 12** but for autumn (SON).

100m Wind SON

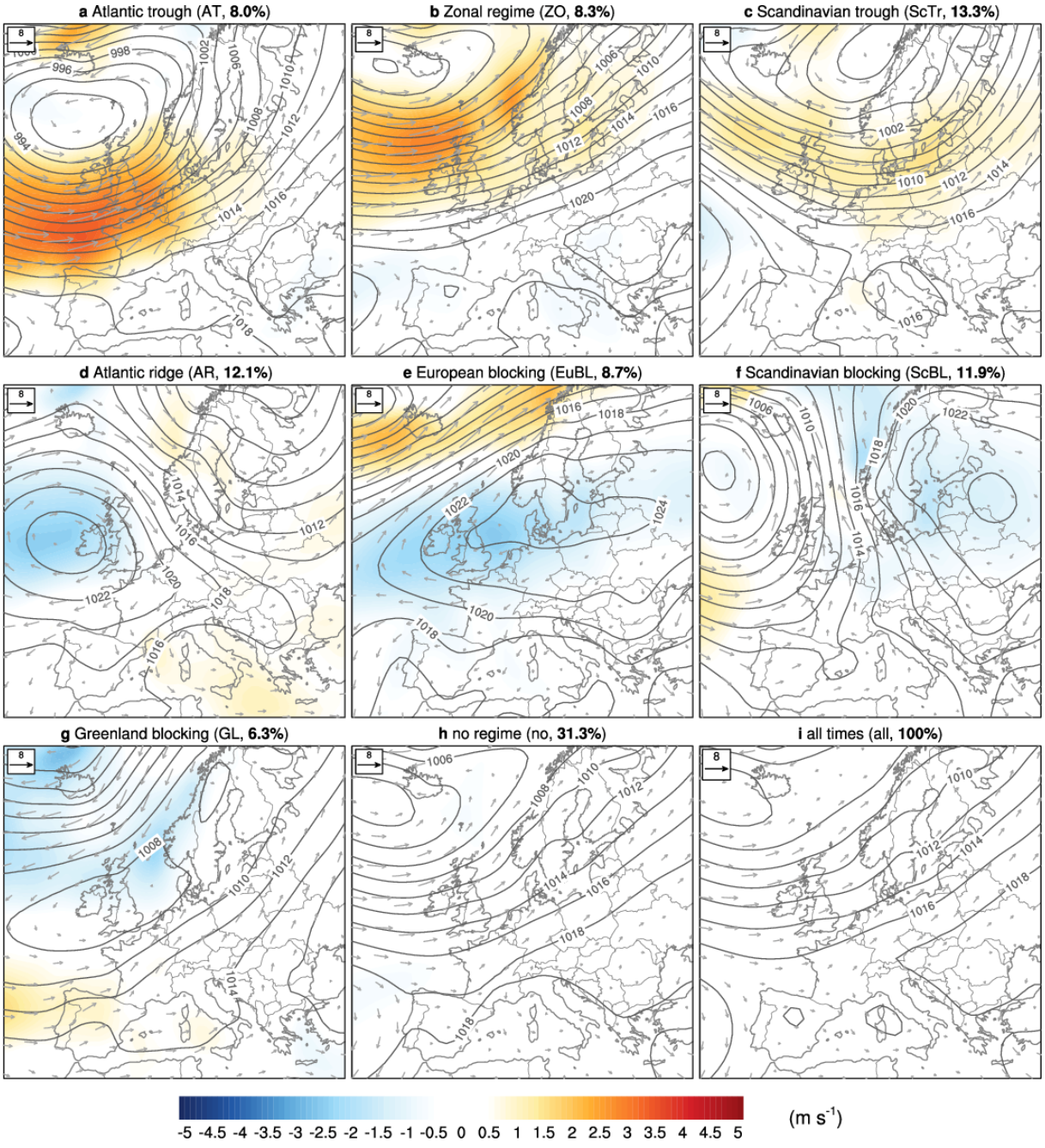

Figure 28: Wind anomalies during the weather regimes in autumn (SON). As

Figure 13 but for autumn (SON).

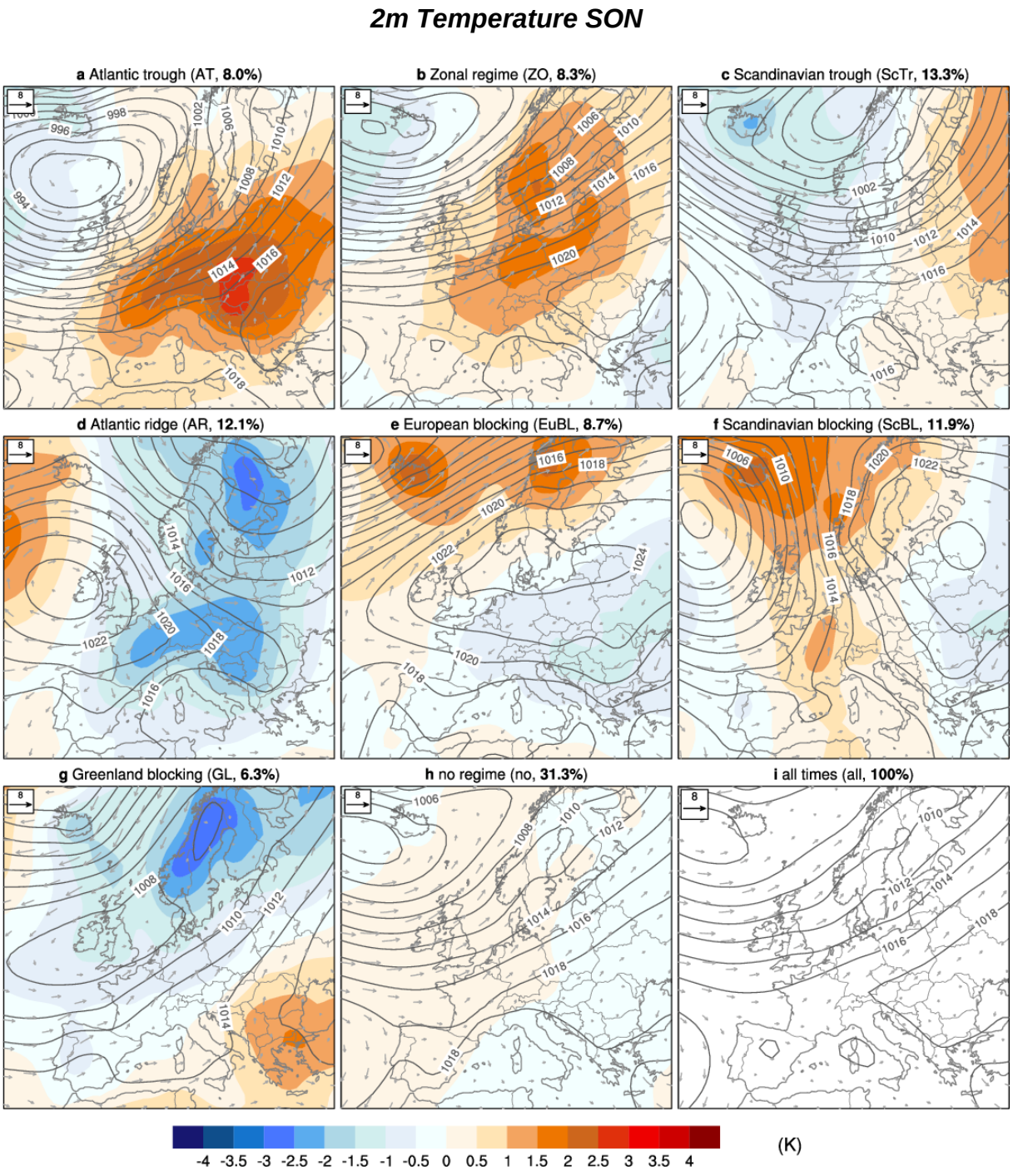

Figure 29: 2m temperature anomalies during the different weather regimes in autumn (SON). As **Figure 14** but for autumn (SON).

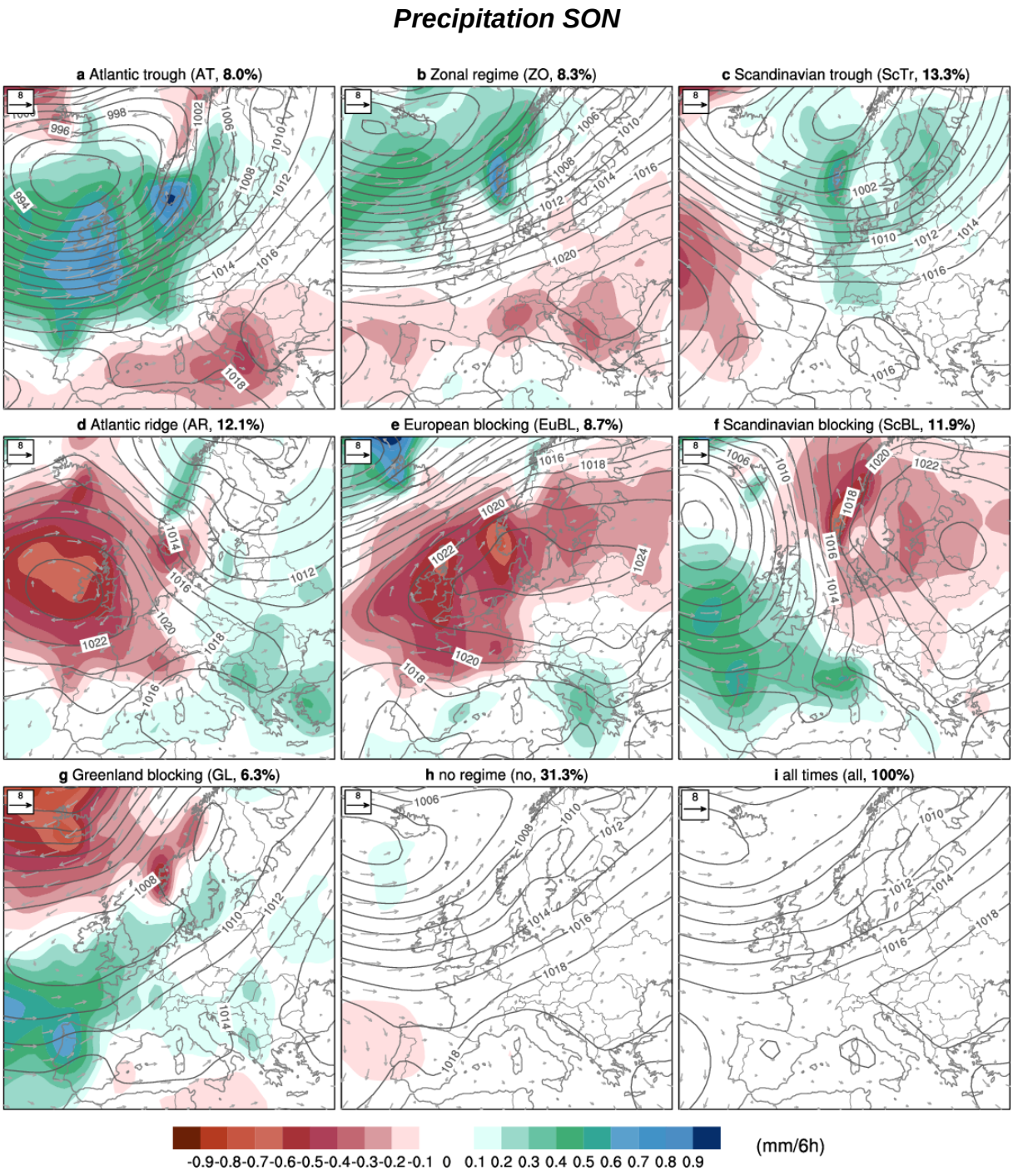

Figure 30: Precipitation anomalies during the different weather regimes in autumn (SON). As **Figure 15** but for autumn (SON).

Fraction of possible Insolation SON

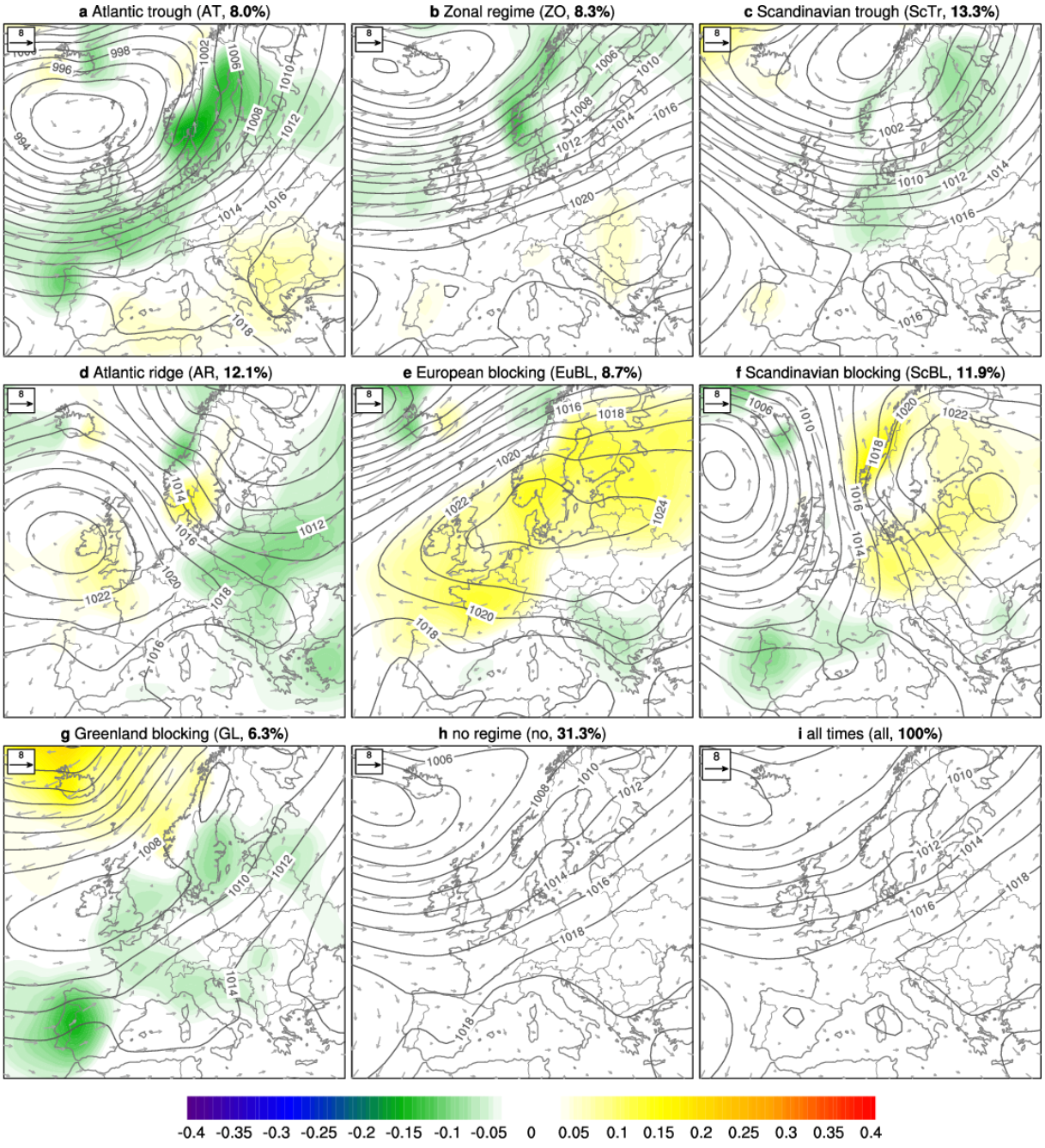

Figure 31: Insolation anomalies during the different weather regimes in autumn (SON). As **Figure 16** but for autumn (SON).

Appendix 2: Modulation of surface weather in the Alpine Region

Here we show surface weather modulation as in Appendix 1 but zoomed on the Central European and Alpine region.

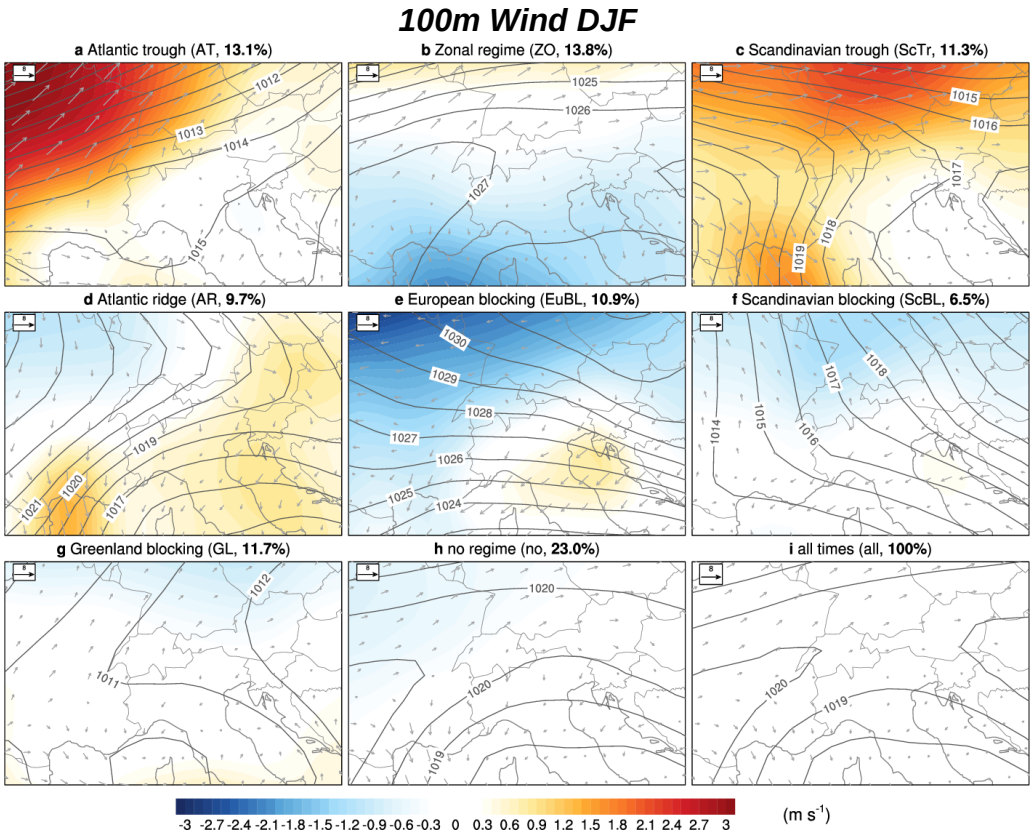

Figure 32: Wind anomalies during the weather regimes in winter (DJF).). 100 m wind speed anomalies (blue-red shading in m s-1), absolute wind at about 100 m (grey vectors), and mean sea level pressure (contours every 1 hPa) for all winter days (DJF) in ERA-Interim (1979-2015) during each regime (a-g), no regime (h), and whole winter (i).

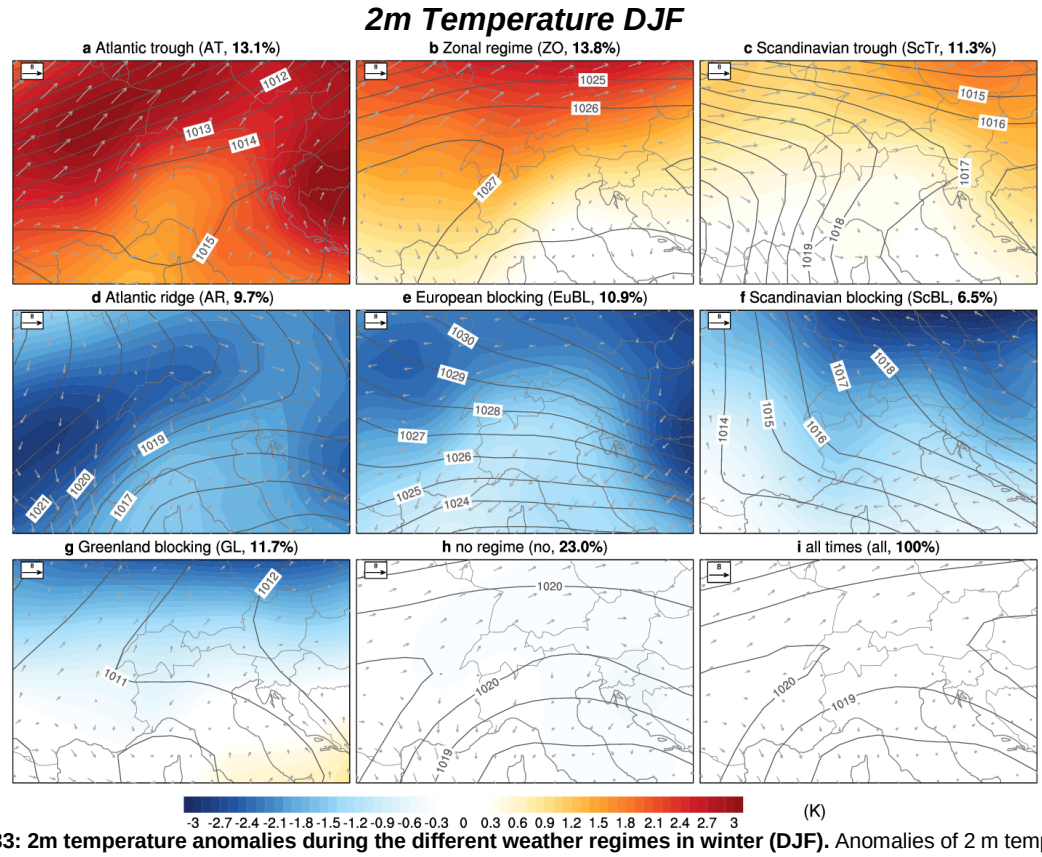

Figure 33: 2m temperature anomalies during the different weather regimes in winter (DJF). Anomalies of 2 m temperatures (blue-red shading in K) computed with respect to the 30-day running average at the respective calendar day, absolute wind at about 100 m (grey vectors), and mean sea level pressure (contours every 1 hPa) for all winter days (DJF) in ERA-Interim (1979-2015) during each regime (a-g), no regime (h), and whole winter (i).

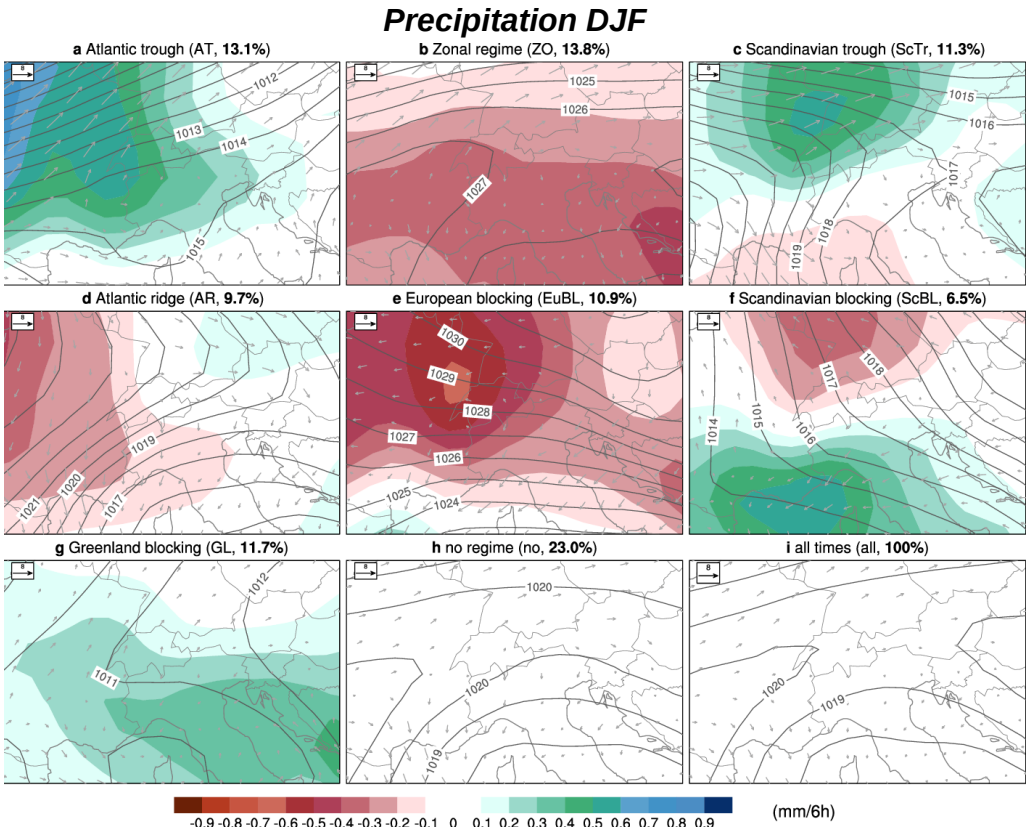

Figure 34: Precipitation anomalies during the different weather regimes in winter (DJF). Anomalies of six-hourly precipitation (red-blue shading in mm $(6h)^{-1}$) computed with respect the winter mean, absolute wind at about 100 m (grey vectors), and mean sea level pressure (contours every 1 hPa) for all winter days (DJF) in ERA-Interim (1979-2015) during each regime (a-g), no regime (h), and whole winter (i).

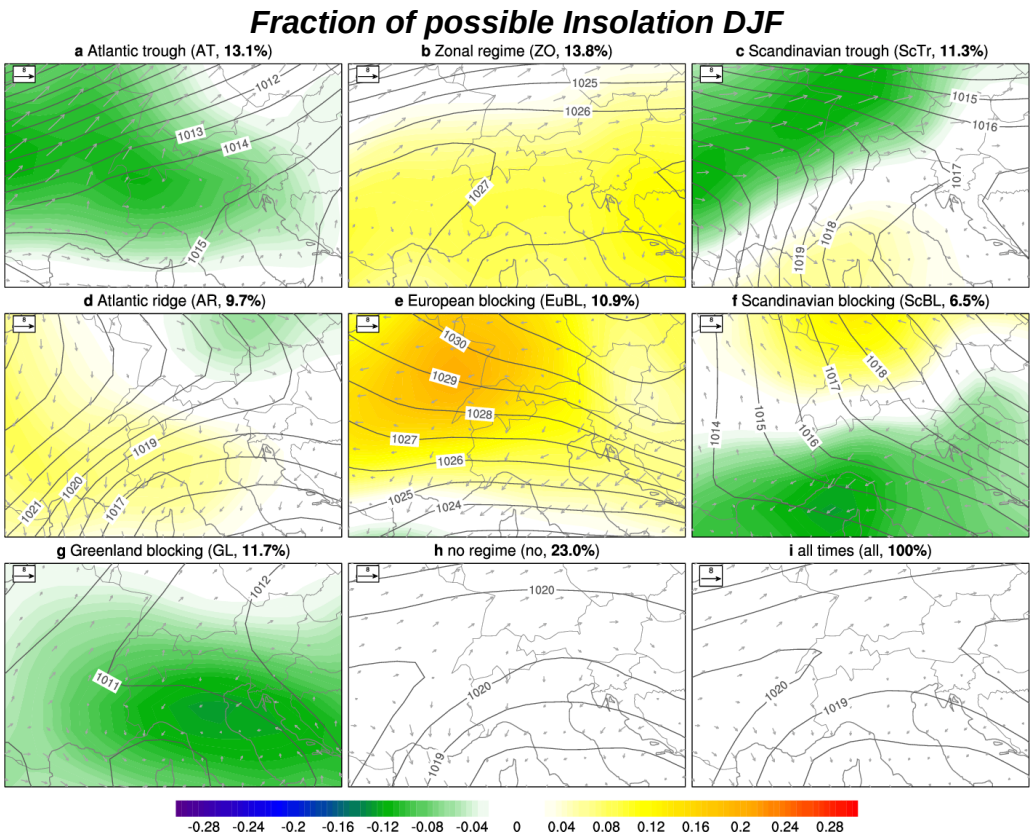

Figure 35: Insolation anomalies during the different weather regimes in winter (DJF). Anomalies of the daily fraction of insolation and daily potential insolation assuming clear skies (green-yellow shading), absolute wind at about 100 m (grey vectors), and mean sea level pressure (contours every 1 hPa) for all winter days (DJF) in ERA-Interim (1979-2015) during each regime (a-g), no regime (h), and whole winter (i).

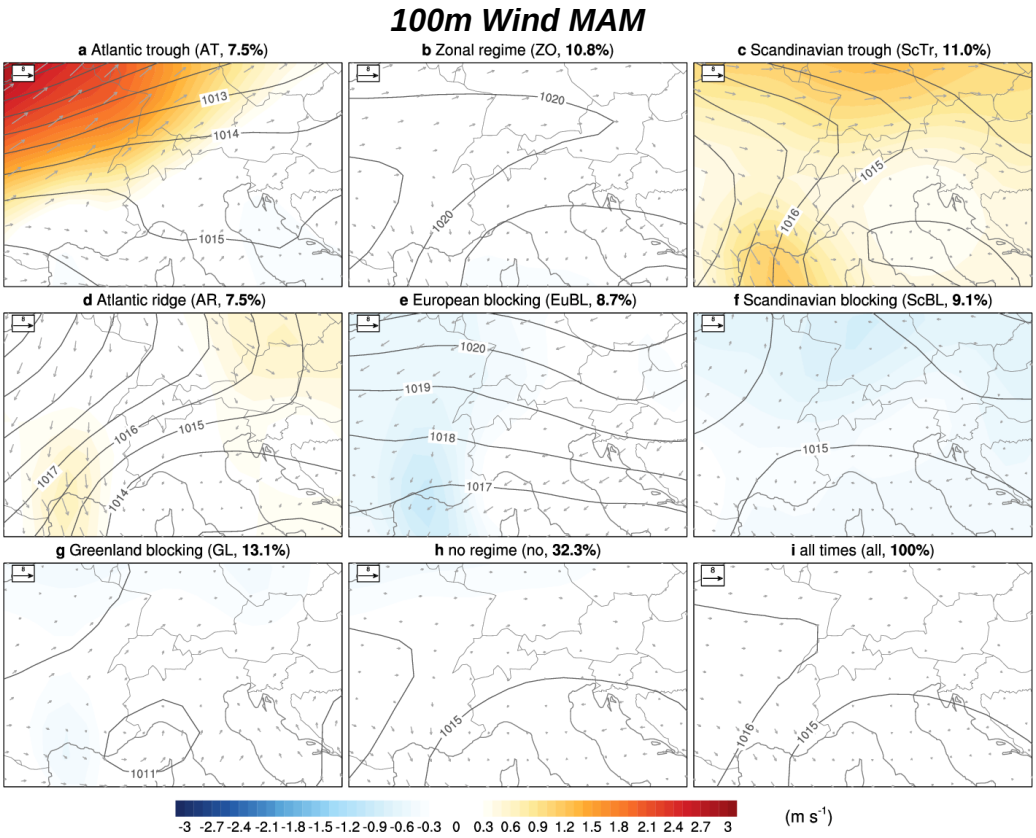

Figure 36: Wind anomalies during the weather regimes in spring (MAM). As Figure 32 but for spring (MAM).

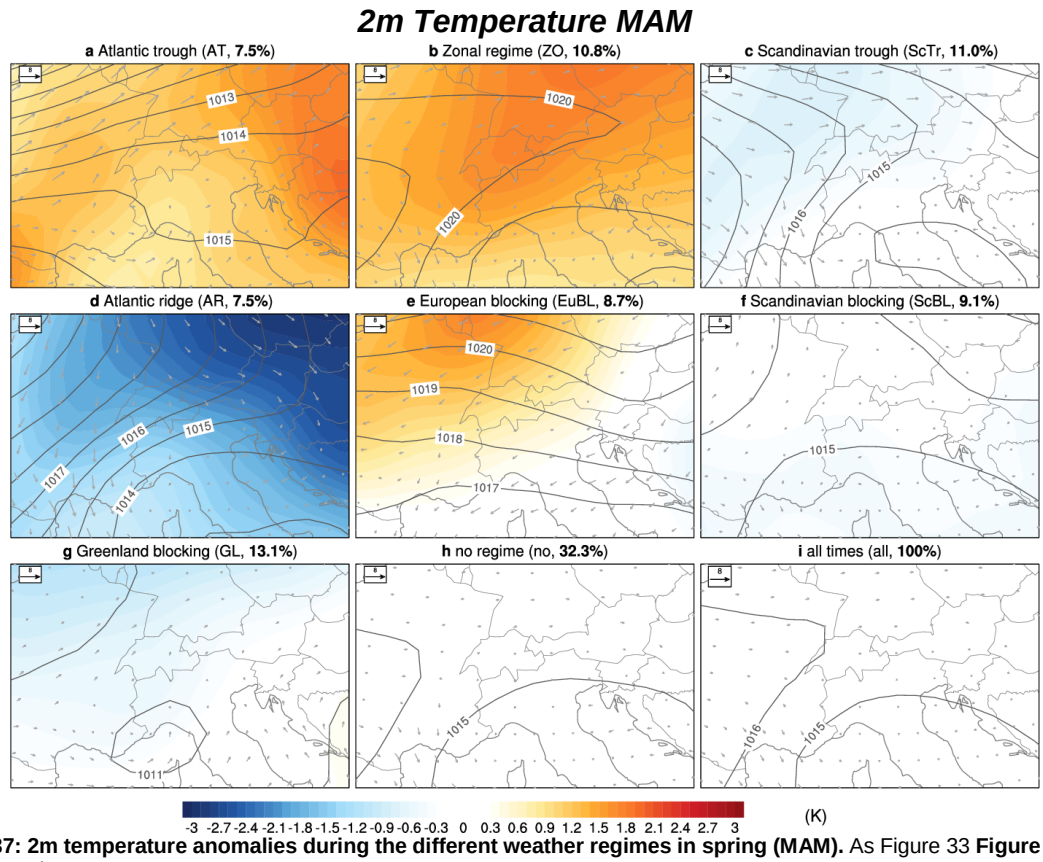

Figure 37: 2m temperature anomalies during the different weather regimes in spring (MAM). As Figure 33 **Figure 32**but for spring (MAM).

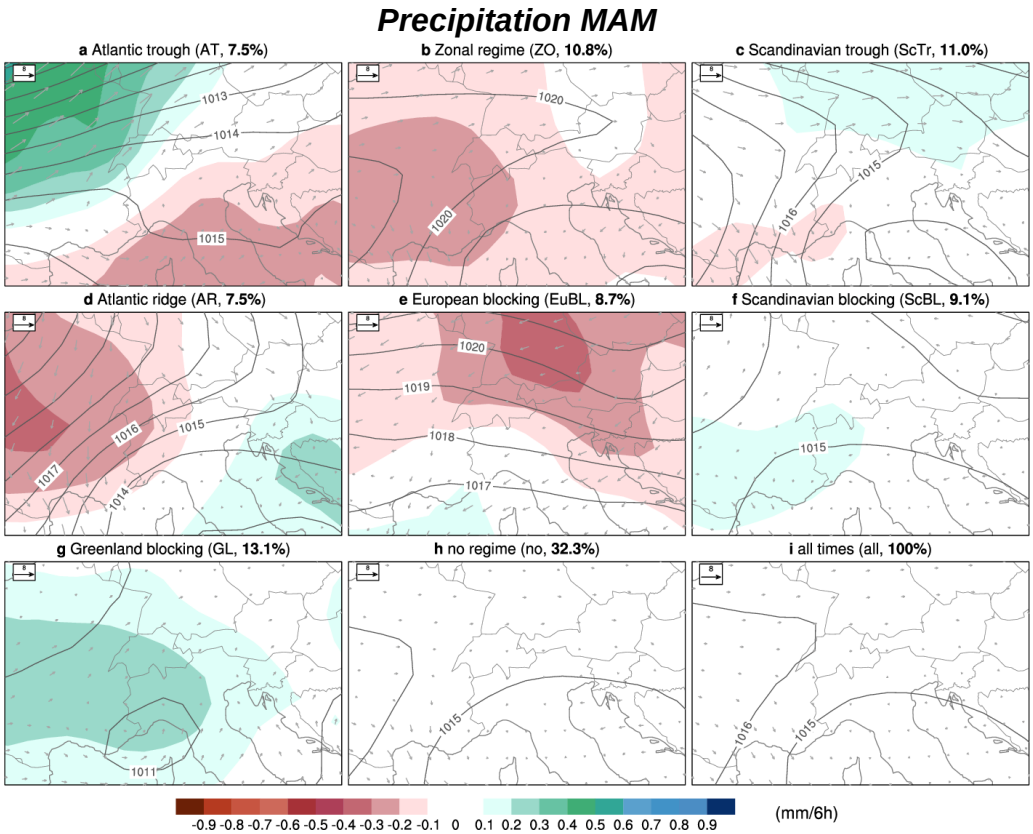

Figure 38: Precipitation anomalies during the different weather regimes in spring (MAM). As Figure 34 but for spring (MAM).

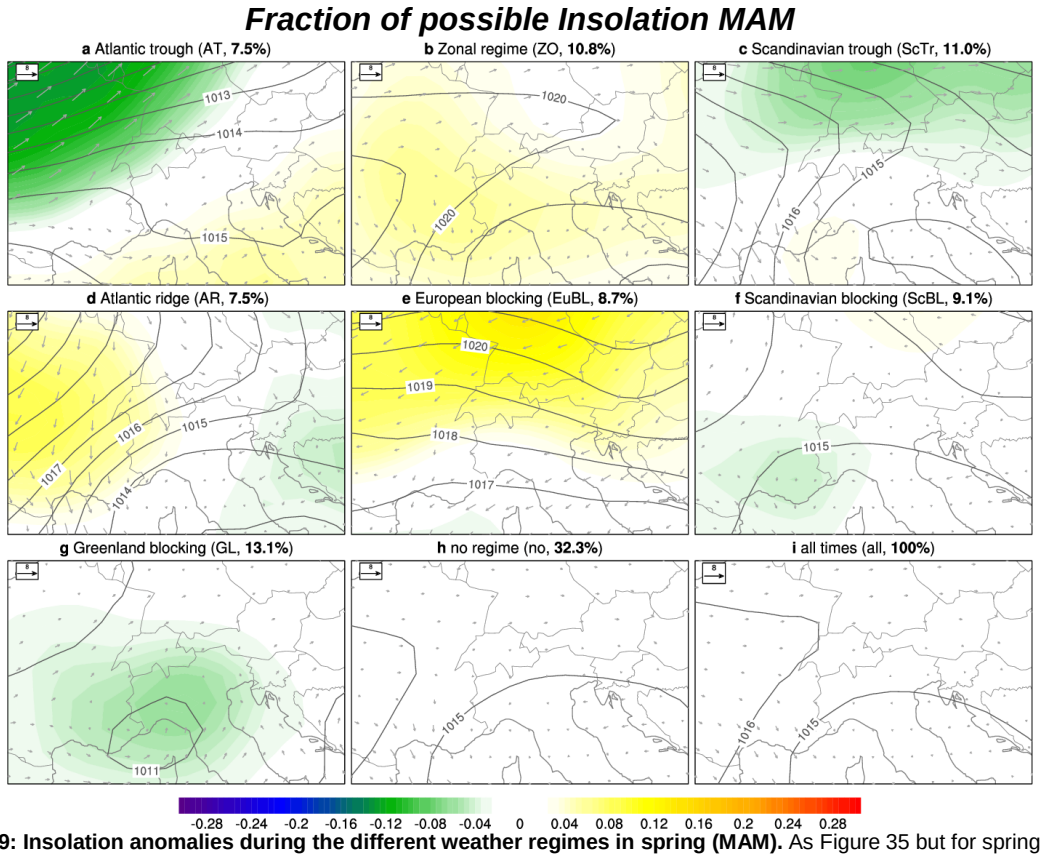

Figure 39: Insolation anomalies during the different weather regimes in spring (MAM). As Figure 35 but for spring (MAM).

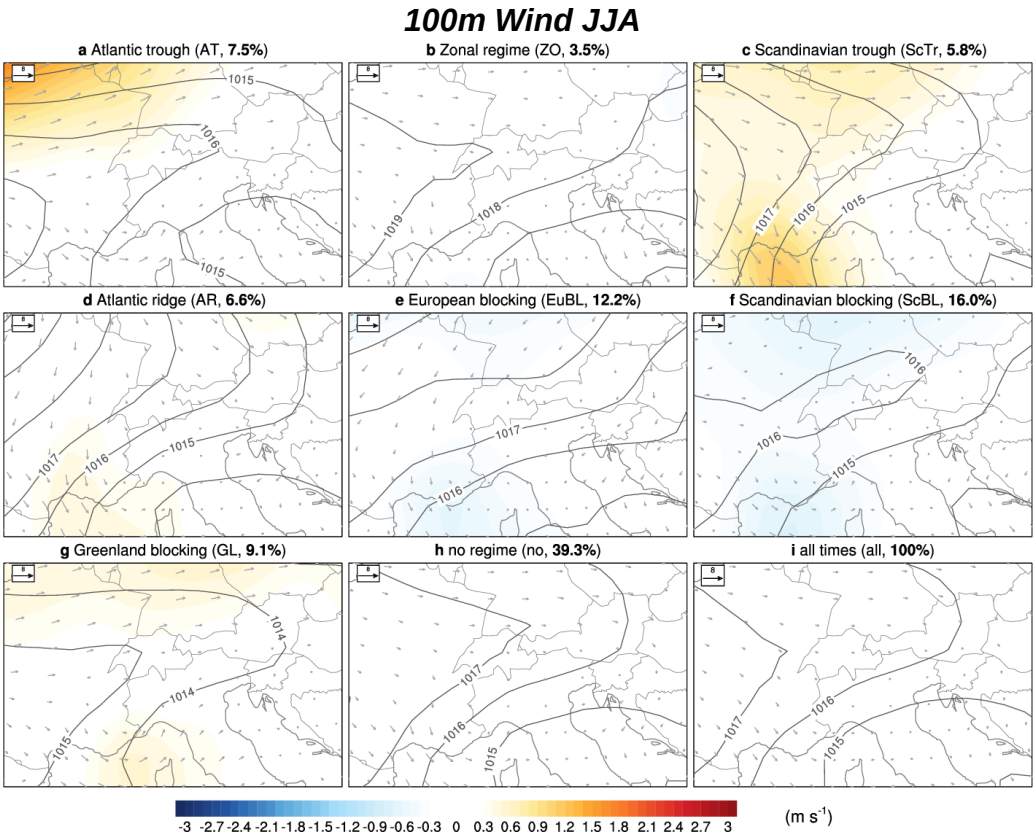

Figure 40: Wind anomalies during the weather regimes in summer (JJA). As Figure 32 but for summer (JJA).

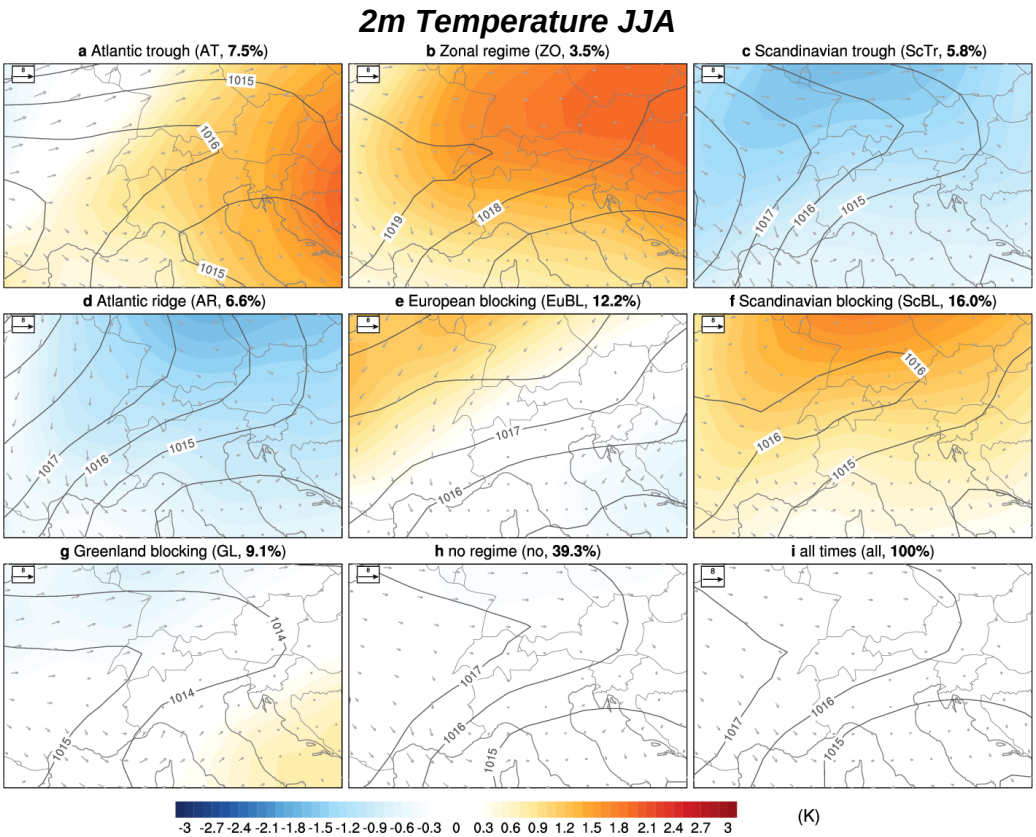

Figure 41: 2m temperature anomalies during the different weather regimes in summer (JJA). As Figure 33 **Figure 32**but for summer (JJA).

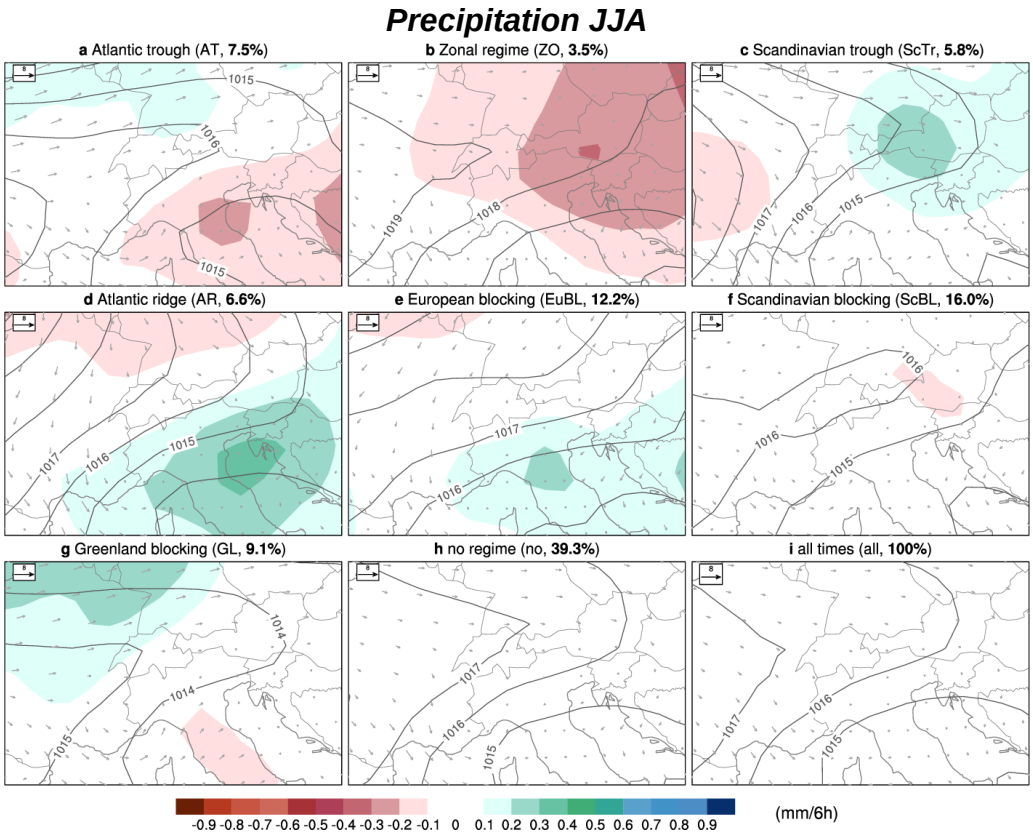

Figure 42: Precipitation anomalies during the different weather regimes in summer (JJA). As Figure 34 but for summer (JJA).

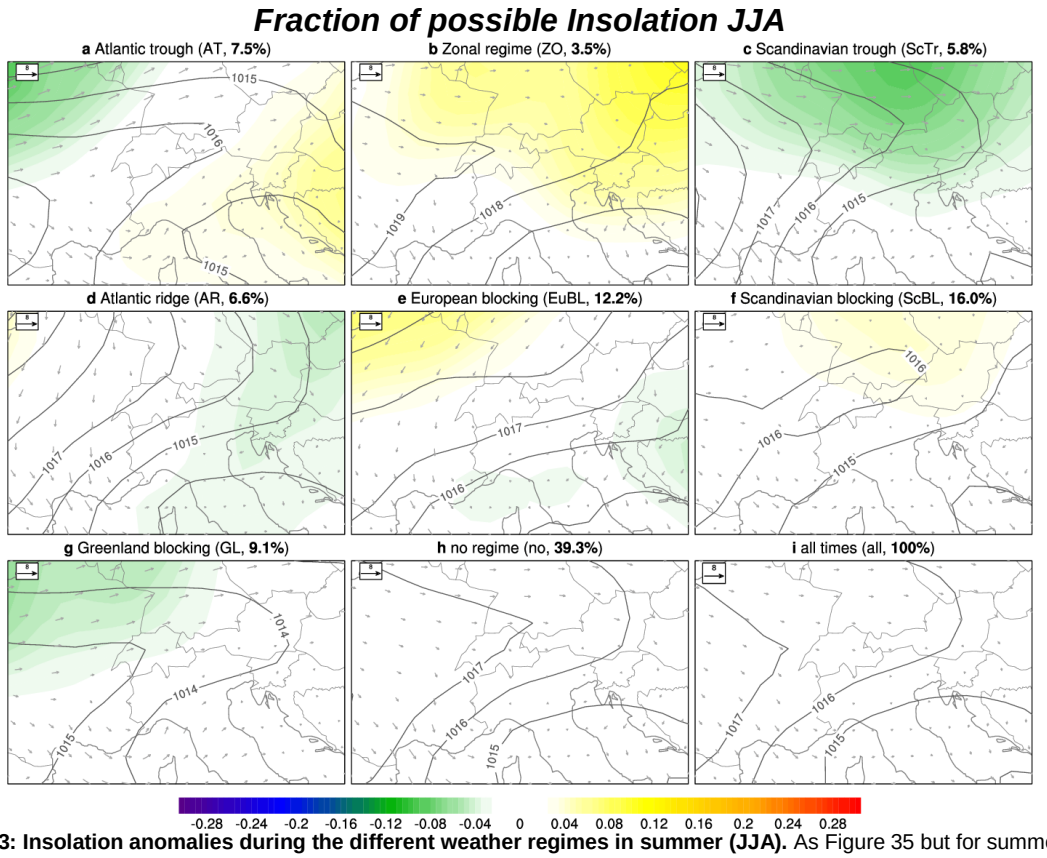

Figure 43: Insolation anomalies during the different weather regimes in summer (JJA). As Figure 35 but for summer (JJA).

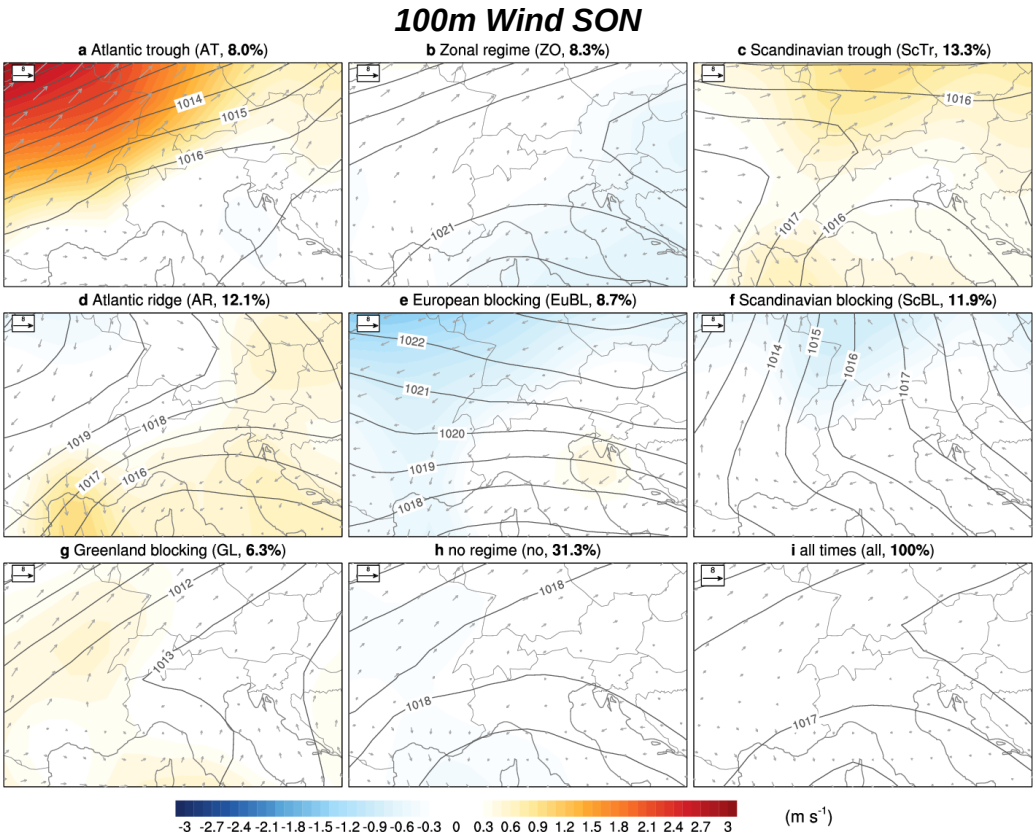

Figure 44: Wind anomalies during the weather regimes in autumn (SON). As Figure 32 but for autumn (SON).

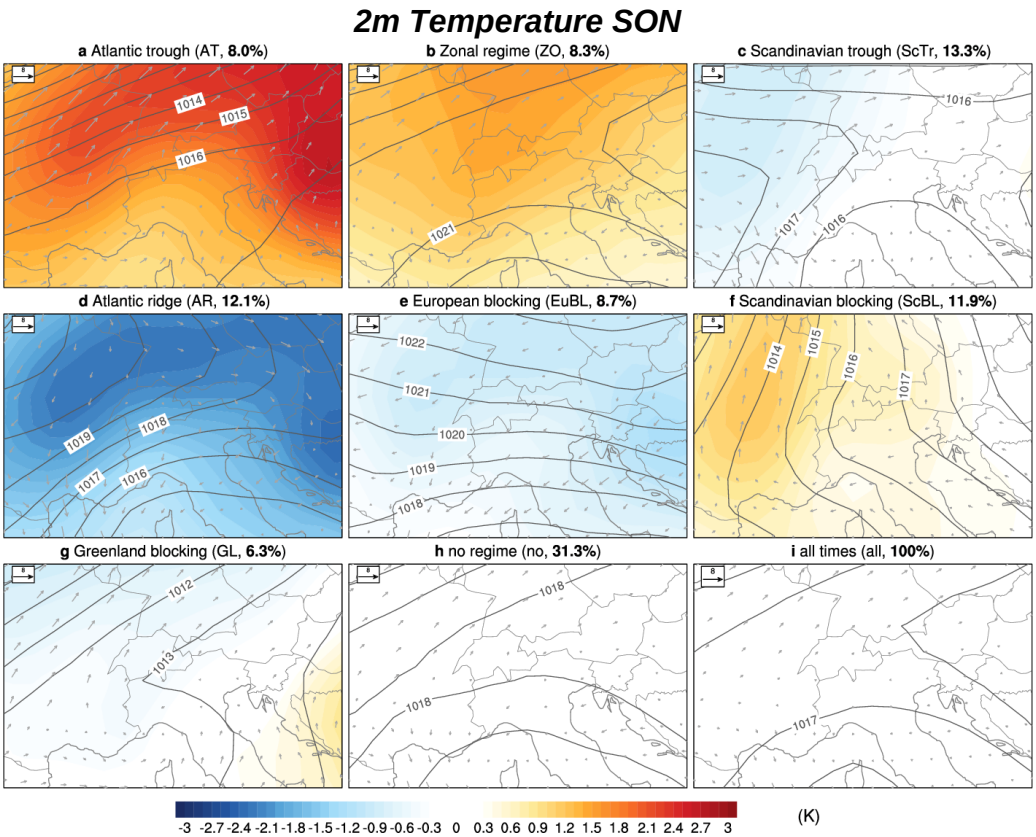

Figure 45: 2m temperature anomalies during the different weather regimes in autumn (SON). As Figure 33 **Figure 32**but for autumn (SON).

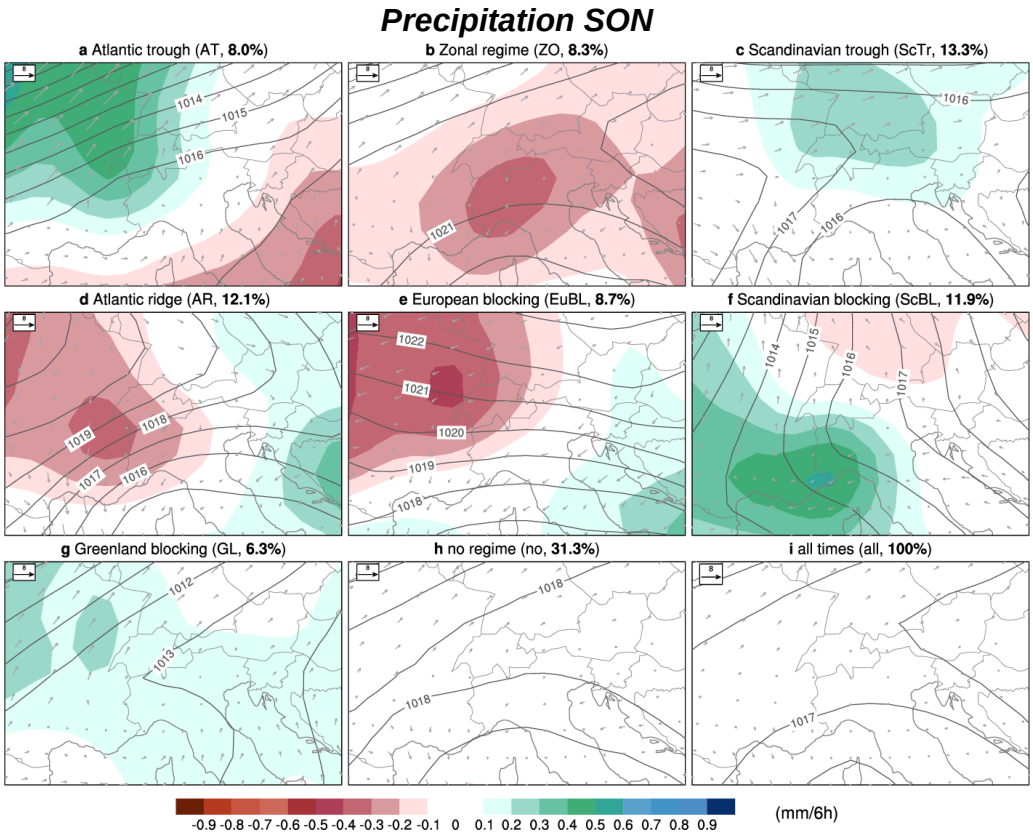

Figure 46: Precipitation anomalies during the different weather regimes in autumn (SON). As Figure 34 but for autumn (SON).

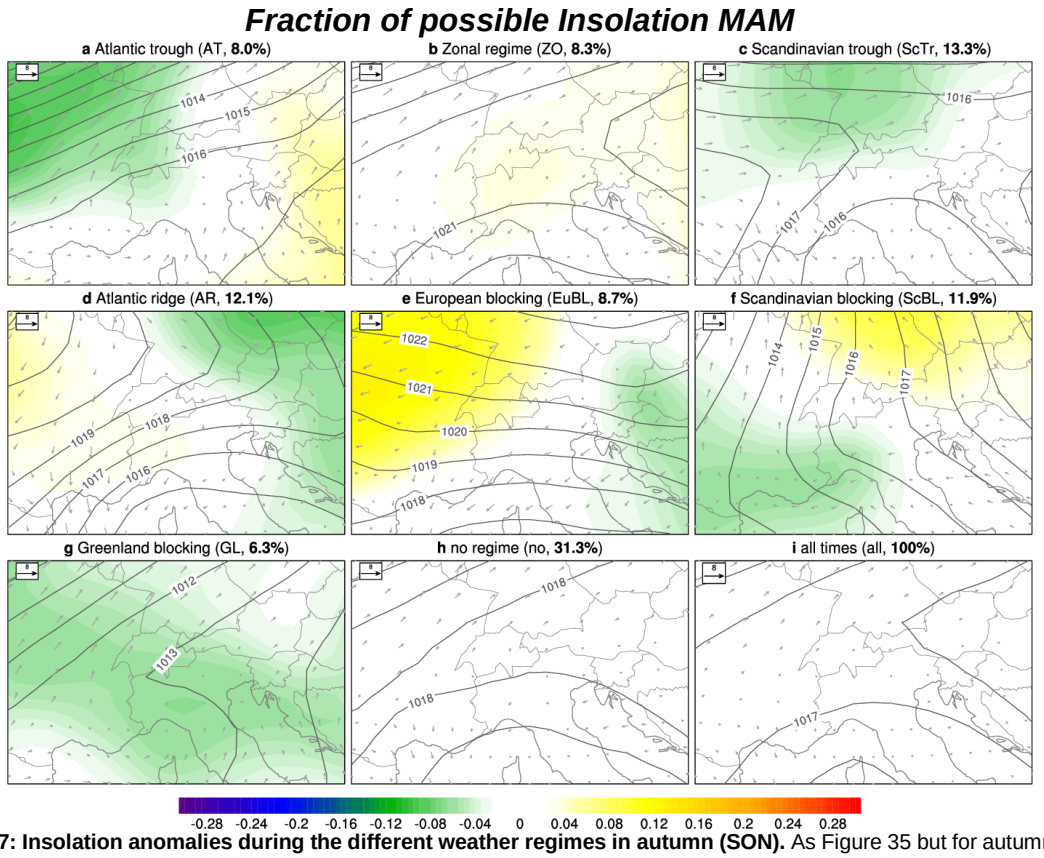

Figure 47: Insolation anomalies during the different weather regimes in autumn (SON). As Figure 35 but for autumn (SON).

References

Barnston, A. G., and R. E. Livezey, 1987: Classification, Seasonality and Persistence of Low-Frequency Atmospheric Circulation Patterns. *Mon. Weather Rev.*, **115**, 1083–1126, doi:10.1175/1520-0493(1987)115<1083:CSAPOL>2.0.CO;2.

Cassou, C., 2008: Intraseasonal interaction between the Madden–Julian Oscillation and the North Atlantic Oscillation. *Nature*, **455**, 523–527, doi:10.1038/nature07286.

Dee, D. P., and Coauthors, 2011: The ERA-Interim reanalysis: configuration and performance of the data assimilation system. *Q. J. R. Meteorol. Soc.*, **137**, 553–597, doi:10.1002/qj.828.

Ferranti, L., S. Corti, and M. Janousek, 2015: Flow-dependent verification of the ECMWF ensemble over the Euro-Atlantic sector. *Q. J. R. Meteorol. Soc.*, **141**, 916–924, doi:10.1002/qj.2411.

Grams, C. M., R. Beerli, S. Pfenninger, I. Staffell, and H. Wernli, 2017: Balancing Europe's wind-power output through spatial deployment informed by weather regimes. *Nat. Clim. Change*, **7**, 557–562, doi:10.1038/nclimate3338.

Jerez, S., and R. M. Trigo, 2013: Time-scale and extent at which large-scale circulation modes determine the wind and solar potential in the Iberian Peninsula. *Environ. Res. Lett.*, **8**, 044035, doi:10.1088/1748-9326/8/4/044035.

Michel, C., and G. Rivière, 2011: The Link between Rossby Wave Breakings and Weather Regime Transitions. *J. Atmospheric Sci.*, **68**, 1730–1748, doi:10.1175/2011JAS3635.1.

Michelangeli, P.-A., R. Vautard, and B. Legras, 1995: Weather Regimes: Recurrence and Quasi Stationarity. *J. Atmospheric Sci.*, **52**, 1237–1256, doi:10.1175/1520-0469(1995)052<1237:WRRAQS>2.0.CO;2.

Papritz L., and Grams C. M., 2018: Linking Low-Frequency Large-Scale Circulation Patterns to Cold Air Outbreak Formation in the Northeastern North Atlantic. *Geophys Res Lett*, **45**, 2542–2553, doi:10.1002/2017GL076921.

Pasquier, J. T., S. Pfahl, and C. M. Grams, 2019: Modulation of Atmospheric River Occurrence and Associated Precipitation Extremes in the North Atlantic Region by European Weather Regimes. *Geophys. Res. Lett.*, **0**, doi:10.1029/2018GL081194. https://agupubs.onlinelibrary.wiley.com/doi/abs/10.1029/2018GL081194 (Accessed January 2, 2019).

Santos, J. A., M. Belo-Pereira, H. Fraga, and J. G. Pinto, 2016: Understanding climate change projections for precipitation over western Europe with a weather typing approach. *J. Geophys. Res. Atmospheres*, **121**, 2015JD024399, doi:10.1002/2015JD024399.

Schaller, N., J. Sillmann, J. Anstey, E. M. Fischer, C. M. Grams, and S. Russo, 2018: Influence of blocking on Northern European and Western Russian heatwaves in large climate model ensembles. *Environ. Res. Lett.*, **13**, 054015, doi:10.1088/1748-9326/aaba55.

Zubiate, L., F. McDermott, C. Sweeney, and M. O'Malley, 2017: Spatial variability in winter NAO–wind speed relationships in western Europe linked to concomitant states of the East Atlantic and Scandinavian patterns. *Q. J. R. Meteorol. Soc.*, **143**, 552–562, doi:10.1002/qj.2943.